REVIEW

Check for updates

Recent advances in the synthesis and catalytic applications of metal–organic framework/ covalent organic framework composites

Yanyan Zhang,†[a] Guilong Lu,†[b] Danfeng Zhao†[a] and Xiubing Huang ⓘ *[a]

The unique characteristics of metal–organic frameworks (MOFs) and covalent organic Frameworks (COFs), such as structural tunability, high specific surface area, and highly organized pores, have led to their widespread application in catalysis. Notably, it is possible to significantly enhance the catalytic characteristics of MOFs or COFs by elaborately integrating them together to overcome the flaws in individual MOFs and COFs, which has been receiving increasing attention. This review starts with a brief overview of the current development of MOF/COF-based catalyst and relative synthetic approaches, followed by a comprehensive and systematic analysis of their applications in photocatalysis, thermocatalysis, and electrocatalysis, involving photocatalytic water splitting, photocatalytic redox reaction, photocatalytic degradation, conventional thermocatalytic redox reaction, and electrocatalytic oxygen reduction reaction. After the above discussion, the prospects and challenges of MOF/COF composites are also proposed.

[a] *Beijing Key Laboratory of Function Materials for Molecule & Structure Construction, School of Materials Science and Engineering, University of Science and Technology Beijing, Beijing 100083, P. R. China. E-mail: xiubinghuang@ustb.edu.cn*

[b] *Laboratory of Industrial Chemistry, Ruhr University Bochum, 44780 Bochum, Germany*

† These authors contributed equally to this work.

Xiubing Huang

Xiubing Huang received his BE (2008) and ME (2011) from the University of Science and Technology Beijing, and his PhD from the University of St Andrews, UK in 2015. He spent one year working at the Research Centre for Materials Science of Nagoya University (Japan) as a postdoctoral fellow. He spent nine months (2019–2020) as a visiting scholar at the research group of Prof. Martin Muhler at Ruhr-University Bochum Germany. Currently, he is a professor at the School of Materials Science and Engineering, University of Science and Technology Beijing. His current research focuses on nanostructured catalysts for organic transformations.

1. Introduction

Nowadays, with the development of the chemical industry, medicine and other industries have risen rapidly, which has also greatly improved the productivity of human society. However, the environmental and energy issues that originate from industrial production are getting worsened, making them one of the issues that need immediate attention. Various nanostructures and their nanocomposites, such as metal oxides, MOFs, metal sulfides, oxynitrides, COFs, and other polymers, have been widely used in the catalysis field. Among them, MOFs composed of organic ligands and inorganic metal nodes as secondary building units (SBUs) through self-assembly have several special advantages, such as highly developed pore structures, ultrahigh surface area, tunable composition and surface properties, and controllable pore size, making them promising catalysts or catalyst supports. Since the first report on MOFs in the mid-1990s, the research and applications on MOF-based materials have grown significantly.[1,2] Similar to MOFs, periodically ordered COFs featured with the powerful interaction of covalent bonds between light elements, such as C, N, O, and B, have drawn great attention owing to their excellent characteristics, such as stable structure, high surface area, adjustable aperture, and adjustable frame, making them very promising for catalysis.[3]

In past decades, MOFs and COFs have developed simultaneously along their individual trajectories. Various MOFs or COFs of different structures and composition can be obtained

by modulating variable parameters (for example, building units, grid expansion, connectivity and functions, or multi-variable strategies).[4,5] To date, more than 90 000 MOFs with >2000 topologies and 500 COFs with >18 topologies have been reported.[6,7] However, the integration of MOFs and COFs into one composite material was first reported only a few years ago.[8] The structural and functional integration of MOFs and COFs can greatly expand their applications and is necessary for an in-depth understanding of structure–activity relationships.[9] The new structures and functions obtained from the hybridization could bring some inspiration to the structural design of MOFs and COFs. For instance, to meet a variety of requirements, researchers frequently add exotic metal sites, such as bipyridine, porphyrin, and phthalocyanine-based metal complexes into COF skeletons.[10,11] These COFs with metal sites often display superior catalytic activity and stability under various reaction conditions compared to MOFs with abundant open metal sites because of the ultrastrong interaction between metal and COFs. The desired nanocomposites should exhibit the properties of both MOFs and COFs if the SBUs of MOFs were incorporated into the building blocks of COFs, which not only enlightens the design and synthesis of MOFs and COFs but also enriches their structures and applications.[12] In addition, the integration can introduce certain innovative functionalities that a single component is unable to do.

The commonality and uniqueness between MOFs and COFs make it possible to build MOF/COF hybrid materials. The porous materials obtained by the combination of MOFs and COFs overcome the inherent weaknesses of a single material and enables their synergistic effects synergy for a wider range of applications. For example, COFs covalently bonded with the surface functional groups of MOFs to form a core–shell structure enable the composite to conduct shell–core mass transfer or MOFs to grow on the surface of COFs, providing a core–shell structure to improve the charge separation efficiency. The research potential of MOFs and COFs in more application sectors has significantly increased as a result of the development of these new composite materials. Based on the properties of COFs and the excellent performance of the original MOFs, the MOF/COF composites have been applied in many fields, such as electrochemistry, environment, biology, and catalysis.[13–15] The integration of MOFs and COFs is a good strategy to optimize the catalytic performance by introducing synergistic effects and eliminating the obstacles of a single component. On the one hand, the porous structure of such composites can provide more active sites and channels for the transport of reactants. On the other hand, due to their
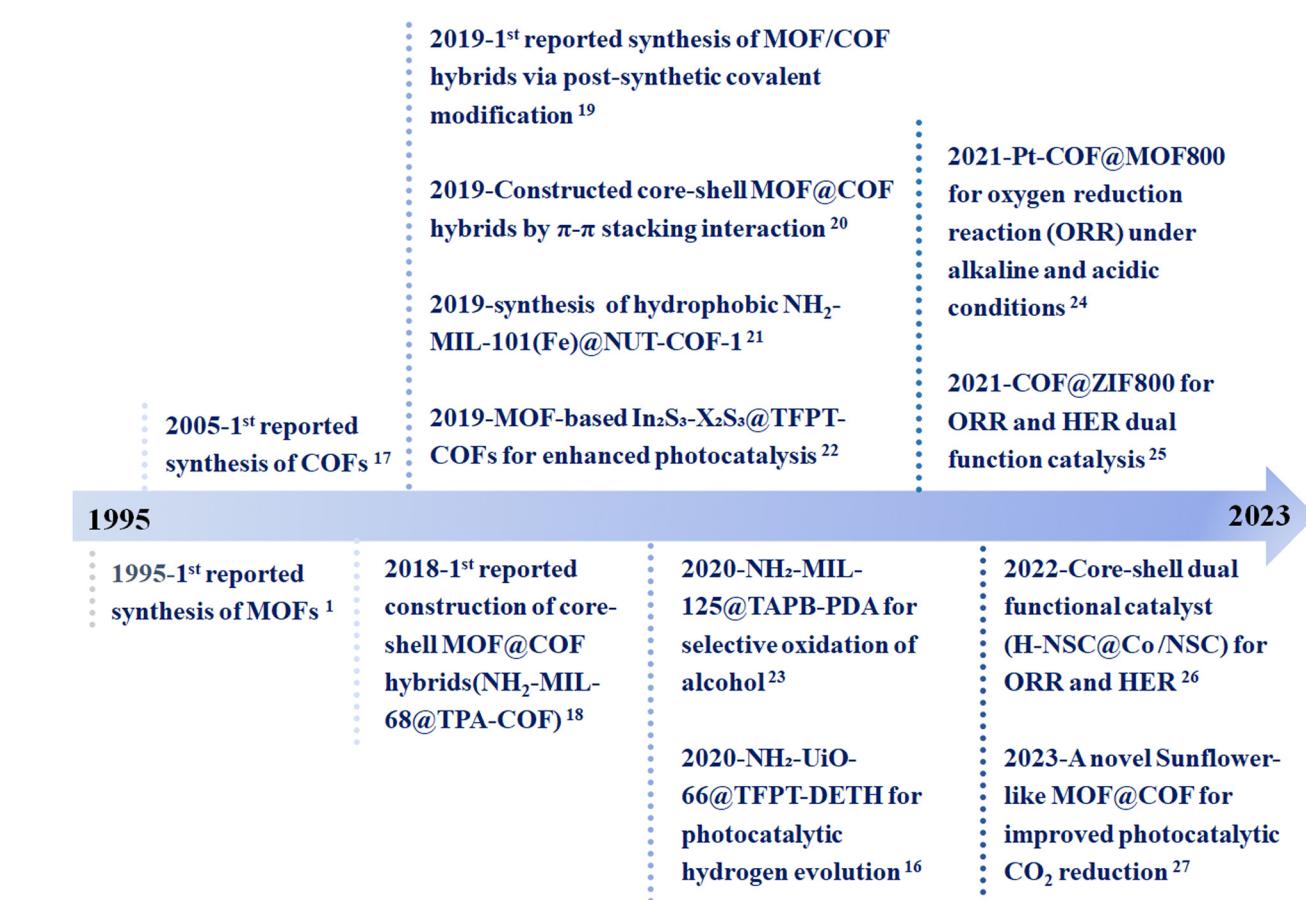

Fig. 1 Timeline of the synthesis and applications of MOFs–COFs.

molecular structure and chemical modularity, strong interfacial interactions can be generated that facilitate charge transfer.[16] Therefore, MOF/COF composites have been greatly developed and applied in the field of catalysis since their appearance. Fig. 1 displays the timeline of the synthesis and applications of MOFs–COFs composites.[2,16–27] Although the application of MOF/COF hybrid materials is very promising, there are still many challenges in this research direction.[16,18,25,28] To date, even though several reviews on the hybrids of MOFs and COFs have been reported,[8,9,12,29–36] they mainly focus on the synthesis strategies and special or comprehensive applications, including photocatalysis, gas separation, sensing, and energy storage. There are still rare comprehensive reviews focusing on the catalytic applications of MOF/COF composites. Therefore, this review focuses on the recent advances in the synthesis and catalytic applications of MOF/COF composites in catalysis, including photocatalysis, thermocatalysis, and electrocatalysis, with the aim to afford an instructive guidance in the rational design of effective MOF/COF composite catalysts (Fig. 2).

2. Synthetic strategies for MOF/COF composites

Since 2016, MOF/COF composites have gradually attracted considerable attention. According to their structures, the present synthetic strategies of MOF/COF composites are broadly categorized into two types: (1) COFs grown on pre-synthesized MOFs. (2) MOFs grown on pre-synthesized COFs. Here, we briefly describe the different synthetic strategies for MOF/COF composites and their corresponding linkage modes.

Fig. 2 MOF/COF composite materials for photocatalytic, thermocatalytic, and electrocatalytic applications.

2.1 COFs growing on pre-synthesized MOFs

It is feasible to build a range of hierarchical MOF/COF structures with varying compositions thanks to the diversity of MOFs and COFs. The integration of MOFs and COFs *via* the imine bond is the most common preparation method. In the first report by Zhang *et al.* using stable NH$_2$-MIL-68 as a substrate for the growth of COFs in 2018, the amino functional groups exposed by NH$_2$-MIL-68 provided abundant anchor sites for the further growth of TPA-COF, and finally a new hybrid material with high crystallinity and hierarchical pore structure (NH$_2$-MIL-68@TPA-COF) was successfully synthesized by two-step modification.[18] In particular, NH$_2$-MIL-68 was first prepared and functionalized with tris(4-formylphenyl)amine (TFPA) to obtain formaldehyde-functionalized NH$_2$-MIL-68, NH$_2$-MIL-68(CHO), which was further coated by TPA-COF nanosheets by covalently linking TFPA and tris(4-aminophenyl)amine (TAPA) through a convenient condensation reaction (Fig. 3a). Using the two-step modification strategy, several other MOF/COF composites using similar aldehydes for surface functionalization followed by condensation reactions of additionally added aldehydes and amines have been successfully synthesized, such as NH$_2$-UiO-66@TDE using 1,3,5-tris-(4-formyl-phenyl)triazine (TFPT) and 2,5-diethoxybenzene-1,4-dicarbohydrazide (DETH),[16] MIL-125-NH$_2$(Ti)@TpTt-COF using 2,4,6-triformylphloroglucinol (Tp) and melamine (Tt),[37] NH$_2$-MIL-101(Fe)@SNW-1 using terephthalaldehyde and melamine,[38] NH$_2$-UiO-66@TpPa-1 using Tp and *p*-phenylenediamine (Pa),[39] as well as IRMOF-3-TpBD using Tp and benzidine (BD).[40] In some cases, the surface functionalization of amine-MOFs with only aldehyde monomers may be not enough for the further condensation reaction. Huang *et al.* proposed a novel seed growth method for the synthesis of NH$_2$-MIL-125@TAPB-PDA composites, in which a low concentration of terephthaldehyde (PDA) and 1,3,5-tris(4-aminophenyl) benzene (PAPB) was first added to form seed particles on the surface of NH$_2$-MIL-125, and then an additional high concentration of PAPB and PDA was added to grow on the seed particles.[23] The thickness of the COF layer can be controlled by the added concentrations of PAPB and PDA in the second step, which can be further functionalized with the antigen galectin-3.[14] The two-step modification strategy has also been modified by first functionalizing amine-MOFs with aldehyde monomers of COFs, and then only amine monomers of COFs were introduced to react with the surface aldehyde groups to form uniform COFs layers on the surfaces of MOFs. Using this modified two-step strategy, several types of MOF/COF composites, such as IR-MOF3@COF-LZU1,[41] aza-MOFs@COFs,[42] NH$_2$-MIL-125@COF-OH,[43] and NH$_2$-UiO-66@Br-COFs,[44] have been successfully prepared. Using PCN-222-Co MOF as the core, the surface of PCN-222-Co can be firstly functionalized with Pa, and then Tp was added for the interfacial growth to form TpPa-1 on the surface to form PCN-222-Co@TpPa-1 composites.[20]

The two-step modification technique, despite making it easier to build a homogenous COF shell on the surface of amine-MOFs, is a little time- and labor-intensive. One-pot synthesis method has been reported for the synthesis of various
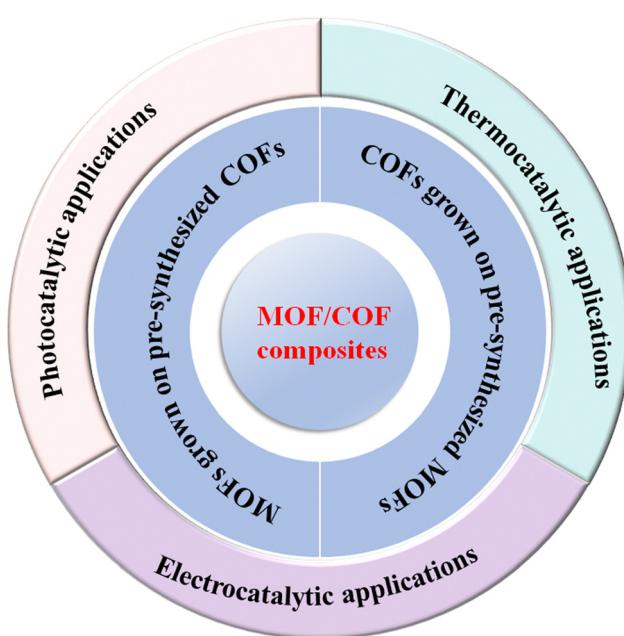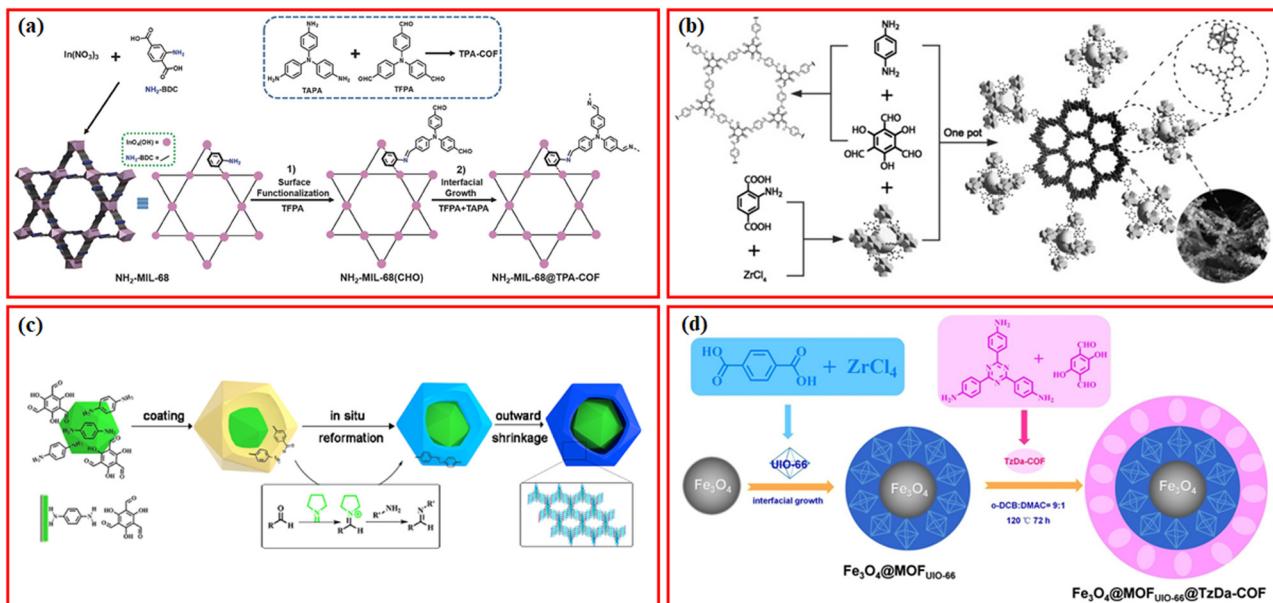
Fig. 3 (a) Schematic illustration of the synthesis of NH$_2$-MIL-68@TPA-COF hybrid material. Reproduced with permission.[18] Copyright 2018, Wiley-VCH. (b) Schematic illustration of the synthesis of NH$_2$-UiO-66/TpPa-1-COF. Reproduced with permission.[45] Copyright 2018, Wiley-VCH. (c) Proposed mechanism of the formation of yolk–shell-structured COF@MOF. Reproduced with permission.[58] Copyright 2021, ACS Publishing Group. (d) Schematic illustration of the magnetic nanocomposite with matryoshka structured Fe$_3$O$_4$@MOF$_{UIO-66}$@TzDa-COF. Reproduced with permission.[61] Copyright 2021, ACS Publishing Group.

MOF/COF composites.[13] Lan *et al.* firstly reported a one-pot synthesis method to synthesize NH$_2$-UiO-66/TpPa-1-COF composites with high surface area, high porosity, and high crystallinity, in which a different proportion of NH$_2$-UiO-66 nanoparticles was added into the synthetic reaction system of TpPa-1-COF with a little more Tp (Fig. 3b).[45] Following the one-pot synthesis method, many MOF/COF composites *via* covalent linkers have been prepared, such as NH$_2$-MIL-125(Ti)@TTB-TTA using 4,4′,4″-(1,3,5-triazine-2,4,6-triyl)tribenzaldehyde (TTB) and 4,4′,4″-(1,3,5-triazine-2,4,6-triyl)trianiline (TTA),[46] H$_2$-MIL-101(Fe)@NUT-COF,[21] NH$_2$-MIL-101@TpMA and NH$_2$-UiO-66@TpMA using Tp and melamine,[47] NH$_2$-UiO-66@TAPT-TP-COF using Tp and 4,4′,4″-(1,3,5-triazine-2,4,6-triyl)trianiline (TAPT),[48] In-MOF-NH$_2$@TP-TA using Tp and TAPT,[49] MTV-Ti-MOF/TpPa-1,[50] NH$_2$-MIL-125(Ti)@TpTta-COF using Tp and TTA,[51] MOF-808@TpPa-1,[52] and Cu-NH$_2$-MIL-125/TpPa-2-COF.[53] *Via* the one-pot strategy, more monomers of COFs besides the aldehydes and amines have been used to prepare COF shells on MOFs, such as 5,10,15,20-tetra(4-pyridyl)-21*H*,23*H*-porphine (TPyP) and pxylylene dibromide monomers for Zr-MOF@Pro-COF-Br.[54] The one-pot synthesis method is relatively facile to prepare MOF/COF composites even using MOFs without –NH$_2$ groups;[15,55,56] however, the uniform coating of COF shells is still challenging. Through consequent treatments such as acid etching, transformation, and shrinkage, yolk–shell structured MOF/COF composites can be formed.[57] For example, a series of the yolk–shell-structured COF@MOF composites with MOFs as the core and COFs as the shell were readily synthesized *via* a template-free solvothermal method, during which the amorphous-to-crystalline transformation and the simultaneous shrinkage of

the shell under the pyrrolidine-catalyzed conditions resulted in the formation of the hollow cavity (Fig. 3c).[58]

With the development of synthesis methods, more functions have been introduced into the MOF/COF composites, such as magnetic separation.[59,60] For example, Fe$_3$O$_4$@MOF$_{UIO-66}$@TzDa-COF with a matryoshka structure was successfully synthesized where UIO-66-MOF was grown on the surface of Fe$_3$O$_4$ nanoparticles to form Fe$_3$O$_4$@MOFUIO-66, which was further coated with TzDa-COF to construct the Fe$_3$O$_4$@MOF$_{UIO-66}$@TzDa-COF hybrid *via* the one-pot synthesis method (Fig. 3d).[61] Several other types of MOFs (NH$_2$-UIO-66, NH$_2$-MIL-125(Ti), NH$_2$-MIL-88(Fe)) were reported to be coated on the surface of Fe$_3$O$_4$ nanoparticles to obtain Fe$_3$O$_4$@MOF *via* the one-pot solvothermal method, which were subsequently coated by COFs using a simple and scalable one-pot room temperature-solution phase method with 1,3,5-benzenetricarboxaldehyde (TFB) and 1,3,5-tris(4-aminophenyl)benzene (TAPB) as monomers.[62] The introduction of magnetic nanoparticles endows these MOF/COF composites with magnetic separation property after applying an external magnetic field, which is promising in practical applications.

Besides the introduction of the magnetic separation function, various kinds of metal nanoparticles or metal ions with high catalytic activity have been also introduced in the structures of MOF/COF composites to prepare core–shell-structured MOF@metal nanoparticles@COF composites or MOF@COF-supported metal nanoparticles or metal ions.[63–65] Metal nanoparticles can be introduced into MOF/COF composites in two main ways. The first is to immobilize metal nanoparticles on the surface of MOFs, followed by coating COFs,[65–68] and the
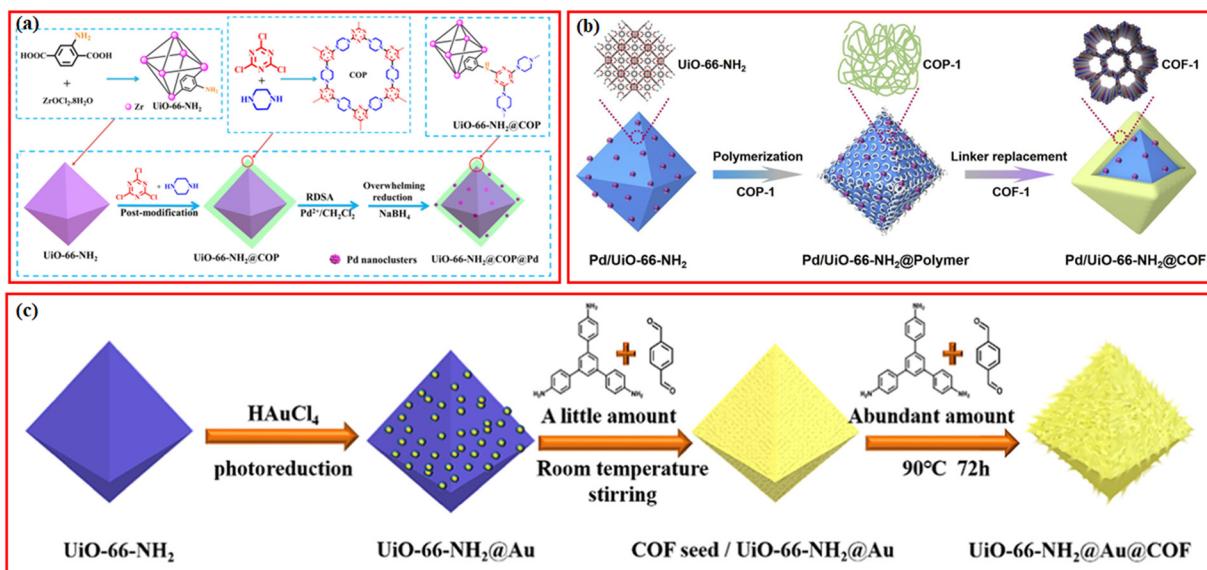
Fig. 4 (a) Schematic illustration of the formation of Pd nanoclusters-doped UiO-66-NH$_2$@COP hybrid material. Reproduced with permission.[70] Copyright 2020, ACS Publishing Group. (b) Schematic illustration for the preparation of the sandwiched Pd/UiO-66-NH$_2$@COF composite. Reproduced with permission.[68] Copyright 2020, Elsevier. (c) Schematic of the preparation process of UiO-66-NH$_2$@Au@COF materials. Reproduced with permission.[63] Copyright 2021, ACS Publishing Group.

second is to directly deposit metal nanoparticles or the reduction of former impregnated metal ions into the MOF/COF composites.[37,69,70] Kim *et al.* prepared the core–shell Pd-doped NH$_2$-MIL-125(Ti)@LZU1 composite.[69] TFB monomers were used to first modify NH$_2$-MIL-125(Ti) and then, *p*-phenylenediamine was added to promote the interfacial growth of LZU-1 COF on the surface of NH$_2$-MIL-125(Ti) to create the NH$_2$-MIL-125(Ti)@LZU1 composite. After the incorporation of Pd^{2+} species into the COF shell, the Pd^{2+} species were reduced to Pd nanoparticles by NaBH$_4$. In another work, covalent organic polymer (COP) was coated on the surface of UiO-66-NH$_2$ *via* covalent linking to form UiO-66-NH$_2$@COP hybrid materials, and the final product, UiO-66-NH2@COP@Pd catalyst, was obtained after anchoring Pd^{2+} species and reduction by NaBH$_4$ *via* the reverse double-solvent approach (Fig. 4a).[70]

Depositing metal nanoparticles or nanoclusters on the surface or COF shell still encounters the possible leakage of metal species during applications and/or pore blockage of the COFs by metal nanoparticles. Confining metal nanoparticles between MOFs and COFs will avoid the possible pore blockage and also endow high dispersion and stability to metal nanoparticles. In addition, the hydrophobic properties of the COF shell can concentrate reactants to the surface of metal nanoparticles for better reaction. Inspired by these advantages, sandwiched MOF@metal nanoparticles@COF composites have been rationally designed and synthesized for targeted applications.[65]

A straightforward method for creating a sandwiched Pd/UiO-66-NH$_2$@COF was proposed by Zeng *et al.*[68] As seen in Fig. 4b, the incipient wetness infiltration approach was used to create the Pd/UiO-66-NH$_2$, which was then functionalized with terephthalaldehyde to create the aldehyde-functionalized Pd/UiO-66-NH$_2$. Then, 1,3,5-tris(4-amidophenyl)triazine was introduced to react with terephthalaldehyde to form an

amorphous nonporous covalent-organic polymer, COP-1, on the surface of Pd/UiO-66-NH$_2$. By substituting 2,5-dihydroxy-1,4-benzenedicarboxaldehyde for terephthalaldehyde, the COF-1 can be converted into COF. The metal nanoparticles can also be deposited on the surface of MOFs *via* photoreduction or *in situ* reduction methods, followed by the seed-growth method for further COF coverage (Fig. 4c).[63,67]

2.2 MOFs growing on pre-synthesized COFs

COFs with nanoporous and 2D structures can also be used as a substrate for growing MOFs to synthesize COF@MOF mixed materials.[71,72] Recently, the Cu$_3$(HHTP)$_2$/TpPa-1 hybrid was prepared using TpPa-1 COF as a support for the loading of 2D conductive Cu$_3$(HHTP)$_2$ MOF (HHTP: 2,3,6,7,10,11-hexahydroxytriphenylene), in which the intimate interaction between MOF and TpPa-1 COF was constructed by the coordination of Cu ions with the carbonyl oxygen and enamine nitrogen groups in MOF (Fig. 5a).[73] Similarly, 2D conductive Ni-CAT-1 MOF was *in situ* grown on a covalent triazine framework (CTF-1) *via* the coordination interaction between Ni^{2+} from Ni-CAT-1 MOF and the dual N sites in CTF-1 layers.[74]

Since the N atoms within the frameworks of COFs have strong coordination ability to metal ions, the coordinated metal ions can provide metal sources for the synthesis of MOFs. Based on this, Caro *et al.* reported a strategy for the construction of TpPa-1@ZIF-67 membranes using an MOF-in-COF concept, in which the prepared TpPa-1 COF layer was immersed in the cobalt precursor to absorb Co^{2+}, and the growth of ZIF-67 could be confined within the structure of TpPa-1 at room temperature *via* the self-assembly of Co^{2+} and 2-methylimidazole (2-meIM) (Fig. 5b).[75] ZIF-67 cells were subsequently formed inside the TpPa-1 pores to create the ZIF-67-in-TpPa-1 membrane, which exhibited excellent potential for gas
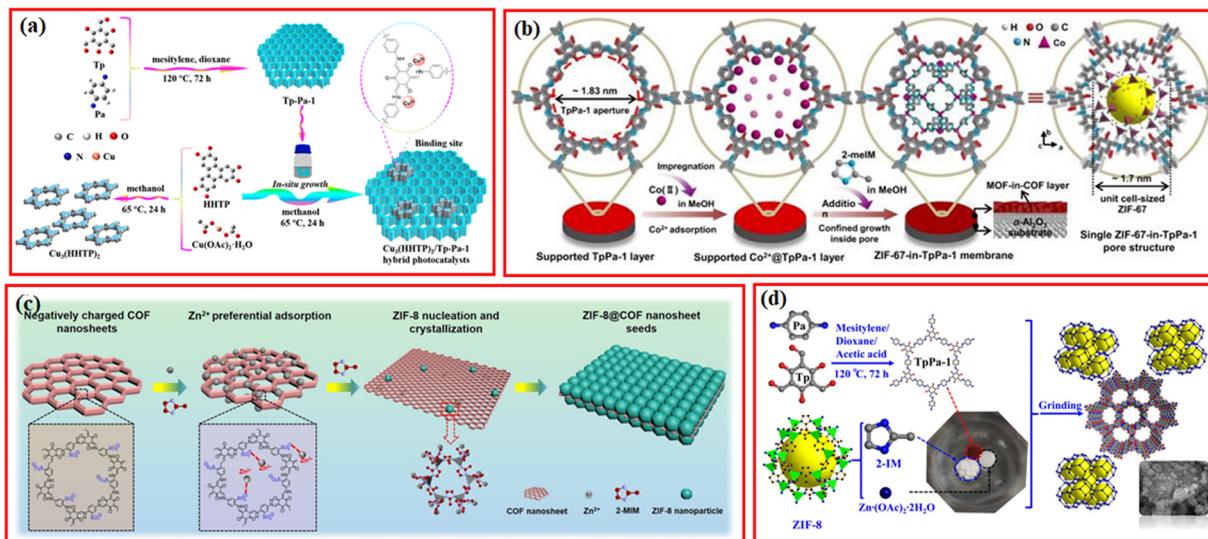
Fig. 5 (a) Schematic illustration for the synthesis of Cu$_3$(HHTP)$_2$/Tp-Pa-1 hybrid. Reproduced with permission.[73] Copyright 2021, ACS Publishing Group. (b) Scheme depicting ZIF-67-in-TpPa-1 membrane synthesis and schematic of the single pore structure. Reproduced with permission.[75] Copyright 2021, Nature Publishing Group. (c) Schematic for the formation of ZIF-8@COF nanosheet seeds, taking negatively-charged TpPa-SO$_3$H COF nanosheet as an example. Reproduced with permission.[77] Copyright 2023, Wiley-VCH. (d) The schematic synthesis of TpPa/ZIF-8-XG. Reproduced with permission.[79] Copyright 2022, Elsevier.

separation. Similarly, ZIF-L-Co MOF can also be *in situ* grown in the pores of nitrogen-enriched TTA-BPDA-COF to form a hierarchical porous TTA-BPDA-COF@ZIF-L-Co hybrid material, in which Co^{2+} species were firstly adsorbed in the channels of TTA-BPDA-COF.[76] To increase the adsorption amount of metal ions within the channels of COFs, Jiang *et al.* proposed an efficient and universal COF induced seeding (COFIS) strategy involving the synthesis of ZIF-8@COF nanosheet seeds for the growth of ultrathin MOF membranes (Fig. 5c).[77] The negatively charged TPA-SO$_3$H COF nanoparticle was mixed with the precursor of ZIF-8, wherein the –SO$_3^-$ group generated strong electrostatic attraction with Zn^{2+}, leading to the preferential adsorption of Zn^{2+} on the surface of COF. The Zn^{2+} enriched on the surface of COF combined with the 2-methylimidazole ligand to generate heterogeneous nucleation on both sides of the COF nanosheet. ZIF-8@COF nanoparticle seeds, whose crystal particles are strongly complimentary, are created by subsequent crystal development.

Unlike the abovementioned synthesis methods, PCN-222-Cu@TpPa-1(1:2) was made using ultrasonic dispersion and vacuum thermal-assisted sequential growth, which resulted in a novel sunflower shape and increased specific surface area and pore size.[27] The pre-synthesized TpPa-1 COF was dispersed in the precursor solution of PCN-222-Cu to adsorb metal ions by ultrasonic dispersion, and then PCN-222-Cu was formed on the surface of TpPa-1 by vacuum heating, forming a novel sunflower type MOF@COF hybrid platform with strong π–π bond stacking. With the co-addition of ZrCl$_4$ precursor, NH$_2$-BDC linker, and acetic acid into the DMF solvent containing a certain amount of TTCOF with 2,4,6-trimethyl-1,3,5-triazine (TMT) and 1,3,5-tris(4-formylphenyl)-triazine (TFPT) as monomers, NH$_2$-UiO-66(Zr) MOF can be formed on the surface of TTCOF after the solvothermal reaction.[78]

Currently, most MOF/COF composites are synthesized by the conventional hydrothermal and solvothermal methods, which requires a long time and a large amount of solvent. Recently, a series of facile methods have been exploited. Su *et al.* prepared TpPa/ZIF-8 composites *via* a simple and fast grinding method in just a few minutes and requires only a slight amount of solvent.[79] By the grinding method, a series of TpPa/ZIF-8 composites with different ratios were synthesized by grinding the synthesized TpPa-1, zinc acetate dihydrate, and 2-methylimidazole in a mortar and pestle for 30 min after the addition of 0.2 mL ethanol (Fig. 5d).[79] Similar to the COFs-coated magnetic MOFs, the COFs can also be coated on magnetic nanoparticles or stainless steel mesh to combine different functions together.[80] For example, Fe$_3$O$_4$@TAPB-COF@ZIF-8 was developed by coating TAPB-COF on Fe$_3$O$_4$ nanoparticles using 1,3,5-tris(4-aminophenyl)benzene (TAPB) and terephthaldicarboxaldehyde (TPA) as monomers, followed by the formation of ZIF-8 on the surface of Fe$_3$O$_4$@TAPB-COF.[81] Unlike the traditional synthesis methods for COFs-supported MOFs, recently, Zou *et al.* reported a new strategy for the fabrication of COF-MOF hybrids *via* the *in situ* functionalization of ligands.[82] CTF-1 were grafted with benzoic acid groups to form B-CTF-1, which was then added into the Ti-MOF reaction system to coordinate with Ti metal clusters by carboxyl groups, resulting in the formation of the B-CTF-Ti-MOF hybrid under the solvothermal conditions.

2.3 Brief summary

In brief, the reported MOF/COF composites mainly included the growth of COFs on pre-synthesized MOFs and the growth of MOFs on pre-synthesized COFs. (1) COFs grown on pre-synthesized MOFs. This method integrates MOFs and COFs mainly through Schiff-based reaction-induced imine bonding.
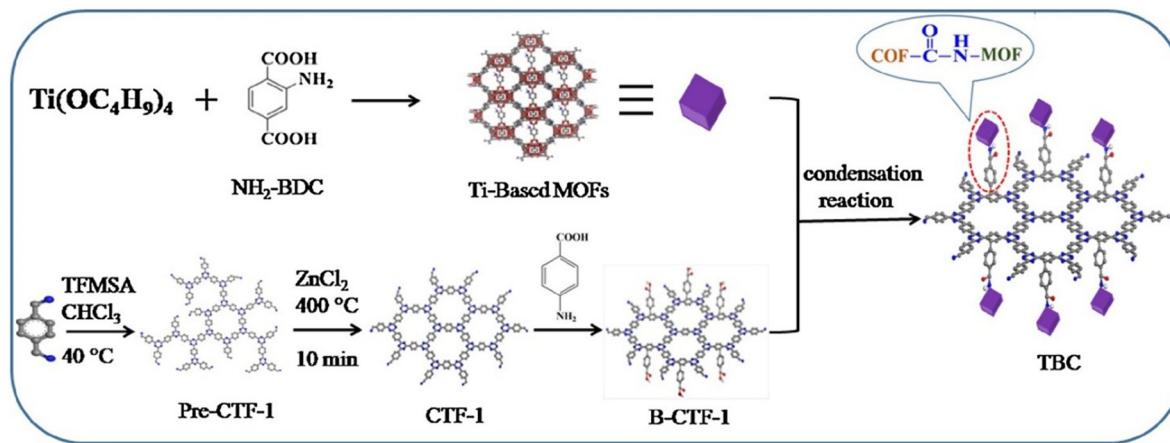
Fig. 6 Schematic of the B-CTF-Ti-MOF composite preparation process. Reproduced with permission.[19] Copyright 2019, Elsevier.

The diversity of MOFs and COFs makes it possible to construct a variety of hierarchical MOF/COF structures, thus laying a solid foundation for their application. However, this approach is somewhat time-consuming and laborious in synthesizing MOF/COF and even suffers from uneven COF shell coating. (2) MOFs grown on pre-synthesized COFs. This method strongly depends on the matching of MOF and COF cell sizes and prepares COF/MOF mainly through covalent and noncovalent bonds, providing a new perspective for the preparation of COF/MOF composite films. However, this method requires a long time and a large amount of solvent for the synthesis of some MOF/COF. During the synthesis process, other functional materials such as magnetic nanoparticles and metal nanoparticles can participate into the MOF/COF composites to afford more functions or better performance. Many methods such as two-step modification method, one-pot synthesis method, and *in situ* growth method have been reported for the synthesis of MOF/COF composites step by step. Even though the MOFs and COFs can be prepared respectively and then combined by vigorous grinding, their poor contact limits their synergistic effects.[83] Recently, a novel NH_2-MIL-125(Ti)/B-CTF-1(TBC) using synthetic covalent modification techniques was successfully prepared by the amide bond.[19] CTF-1 was modified by a benzoic acid fragment to form B-CTF-1, which was then covalently-linked with NH_2-MIL-125(Ti) or NH_2-UiO-66(Zr) by chemically covalent amide bonds (Fig. 6). In addition, besides the MOFs, MOFs-derived graphitic carbon,[84,85] MOFs-derived sulfides,[22,86] and Fe-MOF-derived α-Fe_2O_3,[87] have also been reported as the cores for the coating of COF layers. MOF/COF composites can be further treated to obtain their derivatives for specific applications.[24–26,88,89]

3. Photocatalytic applications of MOF/COF composites

Nowadays, researchers are beginning to pay attention to clean and renewable energy. Photocatalysis, as one of the main applications of solar energy, can realize the conversion of solar energy to chemical energy. In the photocatalytic process, when the catalyst absorbs photons with greater than or equal to the bandgap energy, the electrons in the valence band (VB) are excited to the conduction band (CB), and the corresponding holes are formed in the valence band.[90] These electrons and holes (photogenerated carriers) could react with the reactants when they migrate to the surface of the catalyst. Due to the diversity and designability of the structural units and composition, individual MOFs and COFs have been demonstrated to act as photocatalysts to achieve high photocatalytic performance. MOF/COF hybrid materials can be customized to achieve controllable hierarchical pore, π-conjugated systems, and heterostructures for charge transfer and separation. With their high surface area and ease of modification, MOF/COF composites also offer unique advantages in photocatalysis with diverse and designable band structures to optimize the photocatalytic performance. The unique porous channels can also accelerate the rate of catalytic reactions. In this section, the applications of MOF/COF composites in photocatalytic H_2 production, photocatalytic selective reduction, photocatalytic selective oxidation, and photocatalytic degradation are summarized and discussed.

3.1 Photocatalytic H_2 evolution

In recent years, photocatalytic water splitting into green H_2 is a hot topic in the field of energy research and one of the effective ways to obtain clean energy. The photocatalysts should have good visible light absorption, rapid separation of photoinduced electron–hole pairs, and negative enough reduction potential than H^+/H_2O for creating H_2 to achieve high performance in photocatalytic H_2 evolution. COFs- and MOFs-based photocatalysts have received a great deal of interest in this field due to their long-range organized structure, large surface area, exceptional visible light absorption capacity, and controllable porosity.

For the various reported photocatalytic materials, the integration of covalently-linked MOF/COF heterostructures has great potential. Strong covalent connections in the composites between the MOF and COF not only intimately bind them

together but also serve as a "bridge" for photogenerated electron transport between them during photocatalytic processes. Lan *et al.* first synthesized a covalently-linked NH_2-UiO-66/TpPa-1-COF heterostructured photocatalyst *via* the Schiff base reaction of the $-NH_2$ group in the NH_2-UiO-66 ligand and the aldehyde group in the TpPa-1-COF monomer.[45] Under visible light irradiation, the TpPa-1-COF acts as a light collector to generate photoinduced electrons, which were rapidly transferred to the CB of NH_2-UiO-66 through the covalent bonds to promote the unreversed migration of photogenerated electron–hole carriers (Fig. 7a). In particular, NH_2-UiO-66/TpPa-1-COF (4:6) exhibited the maximum photocatalytic hydrogen evolution rate of 23.41 mmol g^{-1} h^{-1}, which was about 20 times higher than that of the parent TpPa-1-COF. Following this, several different MOF/COF composites linked *via* covalent imine bond between MOFs and COFs have been reported for photocatalytic H_2 evolution, such as NH_2-UiO-66@TFPT-DETH core–shell hetero-frameworks *via* 1,3,5-tris-(4-formylphenyl) triazine (TFPT) and 2,5-diethoxybenzene-1,4-dicarbohydrazide (DETH),[16] NH_2-UiO-66@TAPT-TP-COF *via* 4,4′,4″-(1,3,5-triazine-2,4,6-triyl)trianiline (TAPT) and 2,4,6-triformylphloroglucinol (TP),[48] and graphene oxide-modified NH_2-UiO-66@TAPT-TP-COF.[91] The COF layer can not only increase the visible light adsorption but also reduce the influence of the reaction condition on the MOFs with relatively poor thermal and chemical stability.

Unlike the above MOF@COF, Ma *et al.* reported a series of multivariate PdTCPP ∈ PCN-415(NH_2)/TpPa hybrids for visible-light-driven photocatalytic H_2 production by a covalent integration strategy.[50] Through an *in situ* one-pot synthesis based on ligand bonding, tetravalent Pd-porphyrin ligands were incorporated into PCN-415(NH_2), resulting in multivariate Ti-MOF, PdTCPP ∈ PCN-415(NH_2), which were further coated by TpPa

COF. The obtained multivariate PdTCPP ∈ PCN-415(NH_2)/TpPa exhibited high chemical stability, excellent visible light response ability, good bandgap matching, and effective e–h⁺ separation efficiency. As shown in Fig. 7b, PdTCPP ∈ PCN-415(NH_2) served as an antenna to absorb visible light, and the photoinduced electrons were transferred to $[Ti_8Zr_2O_{12}(COO)_{16}]$ clusters *via* LMCT and then to the LUMO of TpPa through the covalent bond. The electrons concentrated on the Pt NPs surface reduced H^+ to form H_2 with a maximum H_2 evolution rate of 13.98 mmol g^{-1} h^{-1}.

To replace the expensive Pt cocatalysts in photocatalytic H_2 evolution over MOF/COF composites, in Zhang's work, monodispersed transient Cu^{2+}/Cu^+ centers were firstly immobilized by $-NH_2$ groups of NH_2-MIL-125, and then the formed Cu-NH_2-MIL-125 was *in situ* coated by TpPa-2-COF *via* covalent bonding to prepare Cu-NH_2-MIL-125/TpPa-2-COF (Fig. 7c).[53] The cooperation of covalent heterojunctions and monodisperse Cu active sites promoted the migration and separation of photogenerated charge carriers, prolonged the lifetime of excited electrons, and enhanced the active sites for proton reduction, and the optimized Cu-NH_2-MIL-125/TpPa-2-COF (4:6) showed the best H_2 release rate of 9.21 m mol g^{-1} h^{-1}, which was about 17.7 times higher than that of TpPa-2-COF and even higher than the Pt-containing co-catalyst system in different reactions.

The formation of covalently connected MOF/COF hybrid heterostructures is usually completed *via* a Schiff base reaction based on the $-NH_2$ groups of the ligands in MOFs with aldehyde groups from COF reactants. Besides the imine-linked MOF@COF composites, some other interactions were applied to link MOFs and COFs, which also exhibited excellent performance for photocatalytic H_2 production.[82] For example, Zou *et al.* prepared a COF@MOF composite based
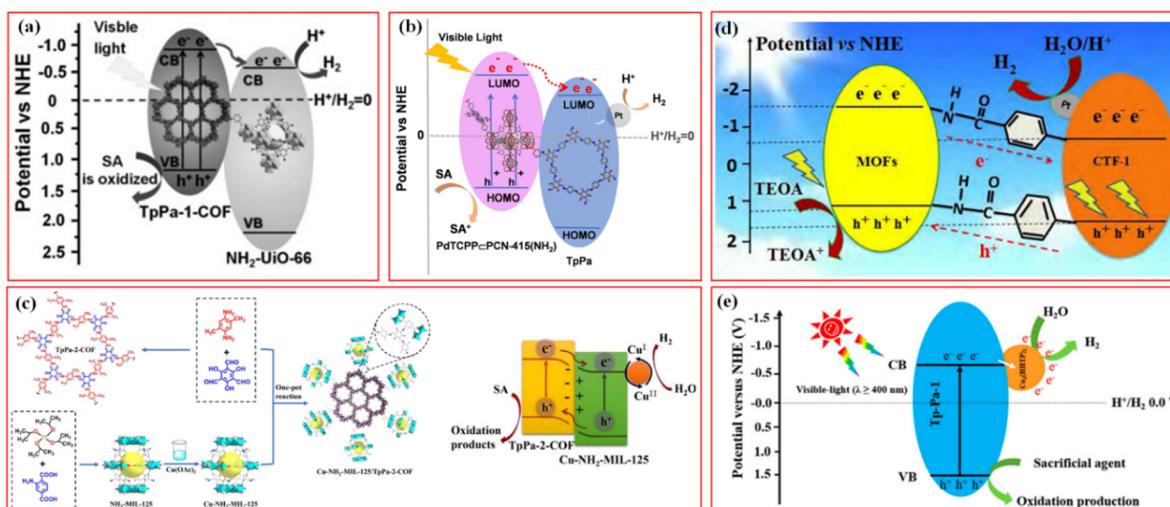

Fig. 7 (a) Mechanism schematic of the NH_2-UiO-66/TpPa-1-COF (4:6) hybrid material. Reproduced with permission.[45] Copyright 2018, Wiley-VCH. (b) The photocatalytic H_2 evolution mechanism of PdTCPP ∈ PCN-415(NH_2)/TpPa hybrids. Reproduced with permission.[50] Copyright 2022, Wiley-VCH. (c) Schematic illustration of the synthesis of the Cu-NH_2-MIL-125/TpPa-2-COF hybrid material and its mechanism in photocatalytic H_2 evolution. Reproduced with permission.[53] Copyright 2022, Elsevier. (d) Photocatalytic mechanism of charge transfer for hydrogen evolution over the 15TBC under visible light irradiation. Reproduced with permission.[19] Copyright 2019, Elsevier. (e) Proposed mechanism for photocatalytic H_2 production by $Cu_3(HHTP)_2$/Tp-Pa-1 hybrid photocatalysts under visible-light irradiation. Reproduced with permission.[73] Copyright 2021, ACS Publishing Group.

on a post-synthesis covalent modification strategy for visible light-driven photocatalytic H$_2$ production.[19] The lipoic acid-modified CTF-1 (B-CTF-1) is covalently attached to NH$_2$-MIL-125(Ti) or NH$_2$-UiO-66(Zr) *via* an amide bond. Under visible light irradiation, the amide bond promotes the separation of electron–hole pairs at the complex interface, and photogenerated electrons could efficiently transfer from NH$_2$-MIL-125(Ti) to B-CTF-1 (Fig. 7d). 15 wt% B-CTF-1@NH$_2$-MIL-125(Ti) catalyzed H$_2$ generation under visible light irradiation with an efficiency of 360 μmol h^{-1}g^{-1}, which is significantly higher than the efficiency of B-CTF-1. Recently, coordinately-linked conductive 2D Ni-CAT-1/CTF-1 with a Z-scheme heterostructure exhibited significantly improved visible-light-driven H$_2$ evolution performance because of the facilitated separation of photogenerated carriers by 2D conductive Ni-CAT-1.[74] In another work, Zhang *et al.* developed a new strategy to construct covalently-linked MOF/COF hybrid materials by the post-synthetic modification of MOFs without –NH$_2$ in metal nodes and ligands.[52] Zr-MOF, MOF-808 without –NH$_2$ ligand, was selected to be ligated with *p*-aminobenzoic acid on the Zr$_6$ cluster of MOF-808. The acetic acid originally coordinated on the Zr$_6$ cluster of MOF-808 was replaced by *p*-aminobenzoic acid (PABA), and the nano-surface of MOF-808 was covered with –NH$_2$ groups. Then, two partially covalently-linked core–shell MOF-808@TpPa-1-COF were synthesized by *in situ* reaction. Typical type II heterojunctions were formed in the MOF-808@TpPa-1-COF (6/4) heterostructured material, showing an H$_2$ evolution rate of 11.88 mmol g^{-1} h^{-1}, which was about 5.6 and 2.6 times higher than that of the parent TpPa-1-COF and the sample without covalent linkage between the two components, respectively.

In contrast to the reported MOF@COF hybrids using COFs to coat MOFs photocatalysts, Wang *et al.* successfully constructed a series of novel MOF/COF heterostructures through the interaction of Cu ions with carbonyl oxygen and enamine nitrogen in Tp-Pa-1 on the surface of Tp-Pa-1 COF (Fig. 7e).[73] This is the first example of application where two-dimensional conductive Cu$_3$(HHTP)$_2$ MOF can be used as a noble metal-free co-catalyst to accelerate the photocatalytic H$_2$ evolution of Tp-Pa-1 COF. The optimized 2D MOF/COF heterostructure exhibited a remarkable photocatalytic H$_2$ evolution rate of 1.76 mmol h^{-1} g^{-1} under visible light irradiation, which is 93 times higher than that of pure TP-Pa-1 COF. Similarly, Tang *et al.* prepared Tp-Pa-2/Cu$_3$(HHTP)$_2$ *via* an easy handling and green mechanochemical method, and the obtained Tp-Pa-2/Cu$_3$(HHTP)$_2$ composite photocatalyst with a mass ratio of 3:1 showed the highest photocatalytic H$_2$ evolution rate of 7.71 mmol h^{-1} g^{-1} as well as good cycling stability under visible light irradiation.[83]

Covalent linkages are often created to connect MOF and COF in the field of photocatalytic H$_2$ evolution to facilitate the separation of photoinduced charge carriers. Even though imine bonds are the most investigated, some other types have also been reported. In addition, to reduce the Pt cocatalysts in photocatalytic H$_2$ evolution, some other transition metal species or conductive MOFs have been used as co-catalysts, which have been demonstrated to be effective routes to improve the performance. Because of the excellent characteristics of MOFs and COFs, they still have a porous structure after lamination even after calcination. The presence of porous structures of MOFs-derived photocatalysts may also allow photocatalytic reactions to occur simultaneously on both the inner and outer surfaces and provides channels and active sites for the transport of reactants, which is still not well studied.[87]

3.2 Photocatalytic selective reduction

Besides photocatalytic H$_2$ evolution, the selective photocatalytic reduction of raw resources such as greenhouse gas CO$_2$ to value-added chemicals and high valence of toxic metal ions to less-toxic metal species or insoluble metal species have also attracted increasing attention in recent years.[92] MOFs- and COFs-based photocatalysts have been exploited for the selective reduction of CO$_2$ to green fuels with high energy density (*e.g.*, CO, CH$_4$, CH$_3$OH, and HCOOH), which also effectively mitigates the global warming issue.[93–95] In the realm of photocatalytic CO$_2$ reduction, MOF/COF composites, with their distinctive porous structure, good CO$_2$ collection capacity, and effective photoinduced charge transfer mechanism, have lately received growing interest.[27,96,97]

Wang *et al.* prepared a series of In, Fe, Zr-MOF@COF hybrids with type-II heterojunction *via* a Schiff-base involved one-pot hydrothermal method.[49] Amid these heterostructures, In-MOF@TP-TA showed the best photocatalytic activity; the CO and CH$_4$ production rate could reach 25 and 11.67 μmol g^{-1} h^{-1}, respectively (Fig. 8a). Considering the strong linear relationship between the CB potentials of specific MOFs and the CO$_2$ reduction efficiency found in further analysis, the unsatisfactory photocatalytic performance of Fe and Zr-based composites was attributed to their relatively positive CB potentials with insufficient reduction ability (Fig. 8b). In fact, Zr-MOFs could be modified by the construction of a typical Z-scheme heterojunction structure with specific COFs for enhanced photocatalytic activity, in which the photoinduced electrons in CB of Zr-MOFs tended to migrate to the VB of COFs due to the relatively narrow potential gap. The quenching of photogenerated holes in the VB of COFs significantly suppresses the recombination of photoexcited electron–hole pairs in COFs, leading to remarkable photocatalytic CO$_2$ reduction performance.

For instance, a porphyrin-based Pro-COF-Br was chosen to hybridize with NH$_2$-UiO-66 to form a direct Z-Scheme nanocomposites for photocatalytic CO$_2$ reduction.[54] The optimal catalysts M@C–Br-1 exhibited the highest CO yield of 106.35 mmol g^{-1} (~2.6 times and 3.2 times higher than of Zr-MOF and Pro-COF-Br, respectively) and CO/CH$_4$ selectivity of 63.17%. However, it should be noted that the co-presence of CO and CH$_4$ commonly causes technical and economic difficulties in product separation and post treatment, which encourages more investigations on developing photocatalysts with more rational reduction capacity for favorable product distribution. Thanks to rapid development in the synthesis of COFs, a novel olefin-linked (C=C) TTCOF prepared by the polymerization of 2,4,6-trimethyl-1,3,5-triazine (TMT) and 1,3,5-tris(4-formylphenyl)triazine (TFPT)
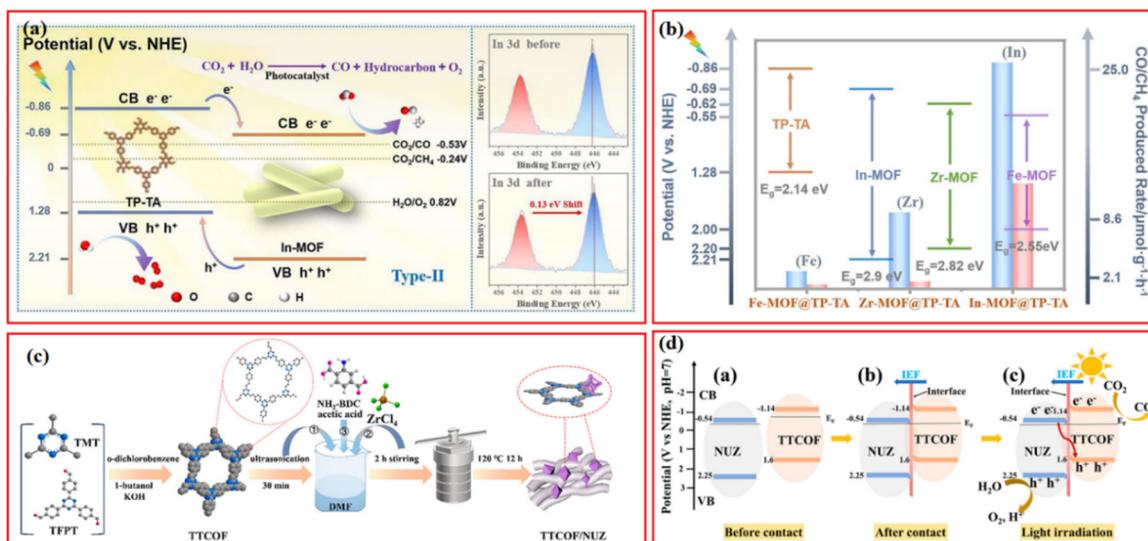
Fig. 8 (a) Mechanism of photocatalytic CO_2 reduction of In-MOF@TP-TA hybrid material and the In-MOF@TP-TA toward before and after photocatalytic reaction from XPS spectra studies (inset) and (b) band-structure diagram and photocatalytic CO_2 reduction activities for TP-TA, In-MOF, Zr-MOF, and Fe-MOF. Reproduced with permission.[49] Copyright 2022, Elsevier. (c) Preparation illustration of x% TTCOF/NUZ (x = 5, 10, 15, 20, 30) composite and (d) schematic illustration of the S-scheme pathway before contact, after contact, and light irradiation for TTCOF and NUZ samples. Reproduced with permission.[78] Copyright 2022, ACS Publishing Group.

not only exhibited superior CO_2 adsorption and reduction ability but also exhibited excellent selectivity toward CO because of its appropriate band structure (Fig. 8c).[78] Niu *et al.* reported a covalently connected Z-scheme TTCOF/NUZ with a remarkable CO yield (6.56 µmol g^{-1} h^{-1}) and a preeminent CO selectivity of nearly 100%. To deeply comprehend the CO_2 reduction pathways, *in situ* FTIR spectra were conducted to detect all possible intermediate products during the reaction. The plausible reaction pathway was proposed by the rational analysis of the variation in the intensity of specific characteristic vibration bands, *i.e.*, $CO_2 \rightarrow CO_2^- \rightarrow HCOOH^* \rightarrow CO^* \rightarrow CO$ (Fig. 8d). More importantly, the photocatalytic reduction of CO_2 experiment in this case was performed in a glass-enclosed gas-circulation reactor. Compared to typical liquid phase reaction process, the gas–solid interface reaction could directly proceed using water vapor as a reductant without any cocatalyst, photosensitizer, and sacrificial agent, which even showed better activity and stability than the liquid homogeneous system.

Yang *et al.* recently found that the CO_2 reduction performance of a gas phase reactor using the same photocatalyst was influenced by the CO_2 concentration. Thus, a lower concentration of CO_2 ($\sim$10% in N_2) is much better than pure CO_2 atmosphere.[79] They also reckoned that the functionalization of COFs shell with hydroxyl groups (–OH) could significantly improve the photoreduction performance of CO_2 due to enhanced CO_2 absorption capacity. In their following comparative experiment, TpPa/ZIF-8-6G functionalized by hydroxyl groups exhibited higher CO generation rates of 84.87 µmol g^{-1} h^{-1} than that of TFPa/ZIF-8-6G (32.56 µmol g^{-1} h^{-1}) without hydroxyl groups. This hypothesis was also validated by another case using NH$_2$-MIL-125@COFs-OH as the photocatalyst.[43]

It is well acknowledged that acetic acid (HAc) is often used as a Lewis acid catalyst to accelerate the formation of COFs nucleus and subsequent growth as well as improve the crystallinity of final COFs materials. Actually, HAc is highly corrosive so that it could controllably decompose NH$_2$-MIL-125 into TiO_2 by precisely tuning its content. Inspired by this concept, the MOF-sacrificed *in situ* acid-etching (MSISAE) strategy was developed for the controllable synthesis of MOF/COF composites including the core–shell MOFs@COFs, yolk–shell MOFs/TiO$_2$@COFs, and hollow-sphere TiO$_2$@COFs nanocomposites.[57] By virtue of co-existence of special three distinct components, yolk–shell NH$_2$-MIL-125/TiO$_2$@COF-366-Ni-OH-HAc possessed Z-scheme heterojunction (COFs/TiO$_2$) and type II heterojunction (MOFs/TiO$_2$), accounting for its remarkable charge transfer and separation efficiency, as well as excellent catalytic performance in photocatalytic reduction of CO_2 in the gas-solid mode. Moreover, the exact role of each functional component in photocatalytic CO_2 reduction reaction was identified, *i.e.*, (1) outer COFs shell improved the light utilization by multiple reflections of incident light; (2) MOFs facilitated the involvement of H$^+$ in CO_2 reduction reaction and enhanced the CO_2 adsorption capability simultaneously; (3) TiO$_2$ promoted the completion of half-reaction (H$_2$O oxidation). Thus, the overall reaction equilibrium could be shifted toward the reduction direction.

All in all, a variety of MOF/COF composites have demonstrated their huge potential in this promising field; meanwhile, many material modification strategies and improvements in the design of CO_2 photoreduction reactor contribute to the further development of this modern technology. However, in contrast to photooxidation and photocatalytic H$_2$ evolution with single electron transfer mechanism, photocatalytic CO_2

reduction is a very complicated reaction involving multielectron transfer process and various adsorbent intermediates. Apart from the strategies for enhanced visible light responsibility and utilization of MOF/COF hybrids, it is also highly desirable in future research to figure out its underlying reaction mechanisms so as to afford a protocol to control the final liquid or/and gas product distribution and even produce more valuable C_2 and C_3 products.

Besides the photocatalytic selective reduction of CO_2, there are some other works on the photocatalytic selective hydrogenation of organic molecules. In addition to combining MOFs with COFs, metal nanoparticles can also be introduced into the MOFs@COFs composite structure, resulting in more exposed active sites, higher conductivity, higher charge mobility, and improved stability of metal nanoparticles. Kim et al. prepared Pd/TiATA@LZU1, in which the amino group in the TiATA core interacted with the aldehyde group of the shell layer LZU1 to ensure the stability of the TiATA@LZU1 core–shell structure, and the imine group of the LZU1 shell layer readily attracted Pd^{2+} to form Pd nanoparticles after reduction (Fig. 9a).[69] Under visible light irradiation, the TiATA core was excited and generated photoinduced electrons while the LZU1 shell acted as an electron mediator to transfer electrons from the TiATA core to the Pd site, promoting the hydrogenation and dehydrogenation of styrene over Pd/TiATA@LZU1 in a continuous-flow microreactor and a batch system.[69] The electron concentration around Pd increases, thus promoting the catalytic reaction of the catalyst under the irradiation of visible light. To solve the blockage and leakage problem caused by metal nanoparticles, Kim et al. further constructed Ti-MOF@Pt@DM-LZU1, in which NH_2-MIL-125(Ti) was used as the catalyst and COF-LZU1 (DM-LZU1) as the hydrophobic shell.[66] The presence of Pt nanoparticles within the Ti-MOF@DM-LZU1 promoted the separation of charge in Ti-MOF, the hydrophobic shell COF was beneficial for the enrichment of reactants, and the interfacial pores acted as nanoreactors to favor the fast electron and mass transport (Fig. 9b).[66] Under illumination, Ti-MOF transferred electrons to Pt NPs with low Fermi energy levels, leading to an increase in the electron density around the Pt NPs, thus improving the photocatalytic hydrogenation performance. In the styrene hydrogenation reaction, the hydrophobic surface trapped styrene into Pt NPs and stabilized the Pt NPs, resulting in stable catalytic performance.

MOF@COF inherits the advantages of parent MOF and COF, but the morphology of MOF and COF affects the performance of the composite. Zang et al. synthesized Ti-MOF@TpTt hybrids coated with ultrathin COF nanobelts with high BET surface area, core–shell structure, and heterojunction by sequential growth.[18] The Pd-decorated Ti-MOF@TpTt catalyst exhibited much higher photocatalytic performance than Ti-MOF, TpT-COF, and Ti-MOF@TpTt hybrid with a fibrous COF shell in the photocatalysis of ammonia-borane (AB) hydrolysis and nitroolefin hydrogenation. During AB hydrolysis, the photogenerated electrons migrated not only from the Ti-MOF core to the TpTt shell under visible light irradiation but were also generated directly on the TpTt shell. The electrons were concentrated on the highly dispersed Pd NPs, enhancing the binding of AB and the activation of water molecules and weakening the B–H bond in AB and the H–O bond in water molecules, which led to the highest hydrogen evolution performance.[37]

The photocatalytic reduction of high-valence metal ions into less-toxic metal species or insoluble metal species for easy recovery have also been attracting great interest.[98–100] MOFs- or COFs-based photocatalysts have been respectively applied for the photocatalytic selective reduction of metal species such as Cr(VI) and U(IV) in recent years.[101–105] Recently, Hu et al. reported that the constructed NH_2-MIL-125(Ti)@TpPa-1 heterojunction via Schiff base exhibited 81.6% photoreduction removal rates of U(VI), much higher than 57.7% of NH_2-MIL-125(Ti) in photoreduction because of the broadened visible light response and improved separation of photogenerated carriers.[106] The photogenerated electrons and $^\bullet O_2^-$ radicals were demonstrated to be the primary reductive radicals while $^\bullet OH$ radicals had some negative influence on U(VI) reduction. The sulfurization of MOFs is another effective modification approach to endow the photocatalyst with new functional moieties and enhanced the optical responsibility, which is often used to prepare desired sulfides for the photodegradation of hexavalent chromium (Cr(VI)) to low-toxicity Cr(III). Considering that metal ion doping (e.g., Bi^{3+}, Sb^{3+}, and La^{3+}) could reduce the bandgap value of specific sulfides as well as the common photocorrosion problem of S–metal bonds, MOF-based In_2S_3-X_2S_3 (X = Bi; Sb)@TFPT-COFs was synthesized by an interfacial design strategy involving an interface ion-exchange method and the amino-functionalization of the heterojunction interface.[22,86] The intimate interface between In_2S_3-X_2S_3 and TFPT-COFs linked by chemical bonds
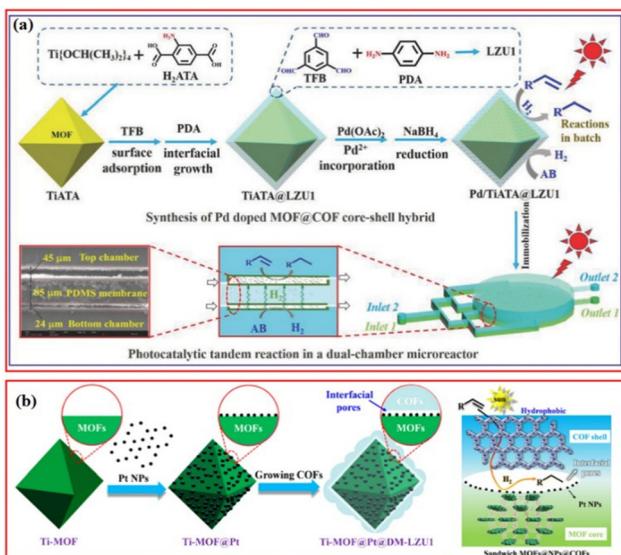
Fig. 9 (a) Schematic scope of the preparation of Pd-doped TiATA@LZU1 core−shell and their photocatalytic applications in batch and dual-chamber microreactor. Reproduced with permission.[69] Copyright 2018, Wiley-VCH. (b) Illustration of the preparation of Ti-MOF@Pt@DM-LZU1 and photocatalytic mechanism. Reproduced with permission.[66] Copyright 2020, ACS Publishing Group.

significantly promoted photoinduced charges transportation and separation so that the complete degradation of Cr(vi) of 30 mg L^{-1} only required 5 min. In contrast to the photooxidation process, Cr(vi) degradation is a reduction reaction without the requirement for ROS, which is usually catalyzed by photogenerated electrons directly.

Photocatalytic reduction over MOF/COF composites is still limited to several reactions. The protecting effect of the COF shell to metal nanoparticles, the electron transfer channels between the MOF and metal nanoparticles, and the excellent visible light response of the COF shell are of great importance in improving the photocatalytic activity and stability. In addition, the pore size and surface hydrophilicity of the COF shell can be tuned for better reactant concentration, reactant/product selectivity, and also mass transfer, leading to improved performance.

3.3 Photocatalytic selective oxidation

Currently, it is widely acknowledged that MOFs and COFs with tunable bandgap structure can serve as robust and controllable reactive oxygen species (ROS) generators to make the oxidation process more selective.[107–109] For instance, Fe-based MOFs comprising abundant Fe–O clusters are often designed to generate hydroxyl radical (•OH) via a Fenton-like route for the activation of stubborn C–H bonds.[110] However, the hydroxyl radical typically exerts negative effects on the target product selectivity due to its ultrastrong oxidation ability. Relatively mild ROS, by comparison, such as superoxide anion radical (•O$_2^-$) and singlet oxygen (^{1}O$_2$), are highly desired oxidants for excellent conversion efficiency and product selectivity.[111] There are many effective strategies for exclusively generating •O$_2^-$ and ^{1}O$_2$; in detail, the incorporation of precious metal porphyrin-based complexes or special element (e.g., Bismuth) with heavy

atom effect is beneficial to produce ^{1}O$_2$. Metal doping, construction of heterojunction, and defect engineering are common strategies for •O$_2^-$ generation.[112] Notably, MOF/COF composites not only inherit their parental structural advantages but also possess more reasonable electronic structure with efficient electron transport channel and potential synergistic effects. To date, a large variety of MOF/COF composites have demonstrated their huge potential in the selective photocatalytic oxidation of organic molecules into corresponding high-value-added products, which would facilitate the transition toward a more sustainable and environment-friendly chemical production mode in the future.[47,113,114]

Since amino-functionalized MOFs were evidenced as powerful platforms to covalently anchor a series of aldehyde-contained conjugated molecules (e.g., methyl red and 2-pyridine-carboxaldehyde) via Schiff base reaction for improved electronic properties and enhanced photocatalytic activity, great emphasis has been put on the elaborate integration of imine-linked MOF/COF composites.[115] A facial and novel seed growth approach was developed to controllably hybridize NH$_2$-MIL-125 with highly conjugated COFs materials (Fig. 10a), in which the outer COFs shell served as a light harvesting center, and photoinduced electrons could rapidly transfer to the inner MOFs Ti–O active sites to activate O$_2$ to •O$_2^-$ through covalent bond bridges between MOFs and COFs (Fig. 10b). The resulting NH$_2$-MIL-125@TAPB-PDA-3 with appropriate COFs thickness exhibited the highest benzyl alcohol conversion rate, which was ~2.5 and ~15.5 times that of the parental MOFs and COFs, respectively. In view of the relatively poor benzaldehyde yield (~15.9%) of its counterpart prepared by the physical mixing of MOFs and COFs, the pivotal role of covalent linkage connection in the improving electron transfer efficiency and hindering recombination of photoinduced carriers was
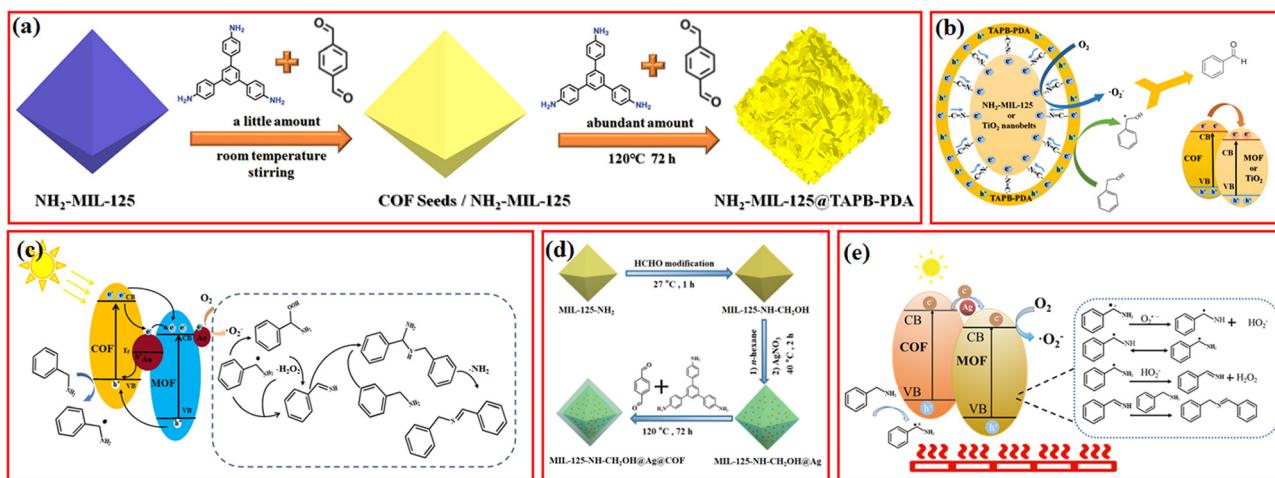
Fig. 10 (a) Schematic of the synthesis process for NH$_2$-MIL-125@TAPB-PDA hybrids, (b) proposed mechanism of the photocatalytic oxidation of benzyl alcohols over NH$_2$-MIL-125@TAPB-PDA-3. Reproduced with permission.[23] Copyright 2020, Elsevier. (c) The proposed mechanism on UiO-66-NH$_2$@Au$_{0.5}$@COF1 for the photocatalytic oxidation of benzylamine. Reproduced with permission.[63] Copyright 2021, ACS Publishing Group. (d) Schematic illustration for the synthesis of the MIL-125-NH-CH$_2$OH@Ag@COF hybrid and (e) schematic illustration of the proposed mechanism for the photothermal catalytic oxidation of benzylamine over MIL-125-NH-CH$_2$OH@Ag-0.5@COF-2. Reproduced with permission.[67] Copyright 2021, Royal Society of Chemistry.

confirmed.[23] Recently, Zhang *et al.* reported that the covalently-linked Cu-NH$_2$-MIL-125/TpPa-2-COF with optimized Cu ions immobilized by the –NH$_2$ groups of MOFs also showed excellent photocatalytic oxidation of benzylamine with high conversion rate (91.2%) and selectivity (>99%) because of the facilitated separation of photogenerated charges and the mono-disperse Cu^{2+}/Cu^{+} active sites.[53]

Considering the unique electronic structure (*e.g.*, localized surface plasma resonance) and superior intrinsic activity of noble metal nanoparticles, plasmonic Au NPs were intercalated into MOF/COF hybrids to serve as hot electron donors and electron transport bridges between the COFs and MOFs simultaneously (Fig. 10c).[63] This advanced structure not only broadens the optical absorption region but also improves the photoinduced carriers' migration efficiency. It was not surprising that the optimal photocatalyst UiO-66-NH$_2$@Au$_{0.5}$@COF1 exhibited excellent activity (66.9% conversion, 96.9% selectivity) and stability toward the aerobic selective coupling of amines to imines compared to its variants, especially UiO-66-NH$_2$@Au and UiO-66-NH$_2$@COF series. In particular, without the protection of the COFs shell, there was a drastic decrease in benzylamine conversion from 61.7 to 41.2% in UiO-66-NH$_2$@Au$_{0.5}$ after 3 cycles. The significance of Au NPs was demonstrated by the relatively moderate photocatalytic activity of all UiO-66-NH$_2$@COF samples toward imine production.[63]

There is no denying that the above MOF@M NPs@COF is still far from producing satisfactory imine yield (>99.9%). In their following investigation, thermo-assisted photocatalysis technology was employed to further improve the catalytic efficiency. A series of MIL-125-NH-CH$_2$OH@Ag@COF hybrids were synthesized by an *in situ* auto-reduction method to form ultrasmall Ag NPs on the MOFs surface, followed by a heterogeneous nucleation method to uniformly grow the COFs shell (Fig. 10d).[67,116] All samples were screened by visible light-driven oxidative coupling of amines at set temperatures (20–60 °C). Based on Arrhenius laws, the benzylamine conversion should increase with increasing reaction temperature in most cases. The experimental results were in agreement with the expectation; in particular, the product yield of MIL-125-NH–CH$_2$O-H@Ag-0.5@COF-2 could reach 99.9% after 12 h visible light irradiation at 60 °C. Given the very poor activity without light illumination, photocatalysis were considered as the main driving force to trigger the catalytic process, whereas external heat is the main promoter to optimize the diffusion of reactants in the reaction system and the adsorption ability of the surface-exposed active sites (Fig. 10e).[67]

In short, the application of MOF/COF composites in photocatalytic selective oxidation is still in a very initial stage; current research only focuses on some primary reactions such as the oxidation of aromatic alcohols and coupling of amines. It is necessary to expand the research scope of oxidation reaction types. In addition, although thermo-assisted photocatalysis has demonstrated its enhanced catalytic performance, the detailed influence of heating in light harvesting sites, ROS generation mechanism, excited electron migration mechanism, and adsorption ability of active sites toward specific reactants is still unclear. Moreover, a possible competition between heat and localized surface plasma resonance of noble metal NPs reported by recent articles could make the whole catalytic system more complicated. Therefore, there is still a long way to go to build a universal and plausible protocol for the design and usage of highly efficient MOF/COF photocatalysts toward selective oxidation in practice.

3.4 Photocatalytic degradation

In recent years, the increasing trend of toxic organic contaminants with low biodegradability has been detected in human daily life-related water source due to irresponsible pollutants emission from industries such as chemical, pharmaceutical, textile, and agricultural. Ion-exchange, physical–chemical adsorption, sorption-catalysis method, coagulation–precipitation, and membrane filtration are examples of conventional technologies that commonly suffer from secondary pollution, high energy consumption, significant operational expenses, and low performance efficiency.[117–119] To ensure the safety and well-being of humanity as well as to restore a delicate ecological balance, great efforts have been made to develop efficient chemical treatment methods for pollutants degradation in a green and efficient manner. Compared to conventional technologies with stoichiometric oxidizing agents commonly suffering from insufficient degradation capacity, secondary pollution, and considerable operating costs, photocatalytic degradation is envisioned as a powerful, environment friendly, sustainable, and energy-efficient technology mainly because of its advanced oxidation processes.[120,121]

Compared with traditional inorganic photocatalysts such as TiO$_2$, MOFs- and COFs-based photocatalysts have attracted remarkable concerns in the photocatalytic degradation of organic pollutants because of their high surface areas, unique structures, and excellent performance.[122] However, the photocatalytic degradation efficiency of pristine MOFs and COFs are still not satisfactory enough because of the limited charge separation and poor visible light response. The visible light-responsive MOF/COF composite materials, among a wide range of developed photocatalysts, have attracted remarkable concerns in the photocatalytic degradation of organic pollutants. Through a rational structural integration and functional modification, the resulting MOF/COF hybrids not only alleviate their intrinsic rapid recombination of photoinduced carriers but also introduce a synergistic effect to further improve the photocatalytic performance. For instance, a pioneering MOF@-COF core–shell photocatalyst (NH$_2$-MIL-68@TPA-COF) exhibited higher photodegradation kinetics of rhodamine B (RhB) than pure NH$_2$-MIL-68 and TPA-COF.[18] Hence, this type of novel functional material possesses enormous potential in the photocatalytic degradation of noxious pollutants in wastewater.

In general, there are two types of heterojunctions, namely, typical type II heterojunction and direct Z-scheme heterojunction, in most reported MOF/COF composites for photocatalytic degradation.[38,41,46,61,123] Taking NH$_2$-MIL88B/TpPa-1 hybrid to exemplify the former one, the photogenerated electrons in the

CB of COFs could rapidly migrate to the CB of MOFs; meanwhile, the photoinduced holes in the VB of the MOFs transfer to the VB of the COFs.[124] Owing to efficient charge transfer in the MOF/COF interface, the recombination rate of the electron–hole pairs can be significantly suppressed, resulting in excellent performance toward the photodegradation of RhB and tetracycline (TC). It is noteworthy that the accumulated holes in the CB should have sufficiently positive potential (>2.7 eV vs. NHE) for the generation of hydroxyl radical ($^\bullet$OH), which is the main reactive oxygen species in most photodegradation processes because of their ultrastrong oxidizing capacity. In this regard, the construction of type II heterojunctions is not suitable and sensible for some MOFs or COFs with specific band structures because photoinduced holes tend to move to a more negative CB in such heterojunctions.

A direct Z-scheme heterojunction was consequently proposed and synthesized to address the abovementioned issue. He et al. reported a covalently integrated NH_2-MIL-125(Ti)/TTB-TTA composite with superior visible light photocatalytic ability in eliminating the organic dye methyl orange

(MO) and colorless phenols.[46] Due to its unique matching mode of MOFs and COFs, it is the photoinduced electrons in the CB of the MOFs that transfer to the VB of the COFs, leading to the spatial charge separation by combination with photogenerated holes in the CB of the MOFs (Fig. 11a). In this case, abundant electrons and holes were accumulated in the CB of COFs for the activation of dissolved O_2 to $^\bullet O_2^-$ and the VB of the MOFs for the production of $^\bullet$OH, respectively. Impressively, no noticeable decrease was found in the photodegradation performance after several cycles, and NH_2-MIL-125(Ti)/TTB-TTA still maintained its morphological and chemical structure as well. The excellent durability and stability of the photocatalyst were attributed to the protection effect of the COFs shell against photocorrosion and deactivation. To some extent, this research opened an avenue toward the construction of similar well-connected MOF/COF hybrid materials for application in photocatalytic degradation and wastewater treatment. A series of similar Z-scheme photocatalyst systems have been reported in the past few years, for example, NH_2-MIL-88B(Fe)/TPB-DMTP-COF composite for the degradation of sulfamerazine
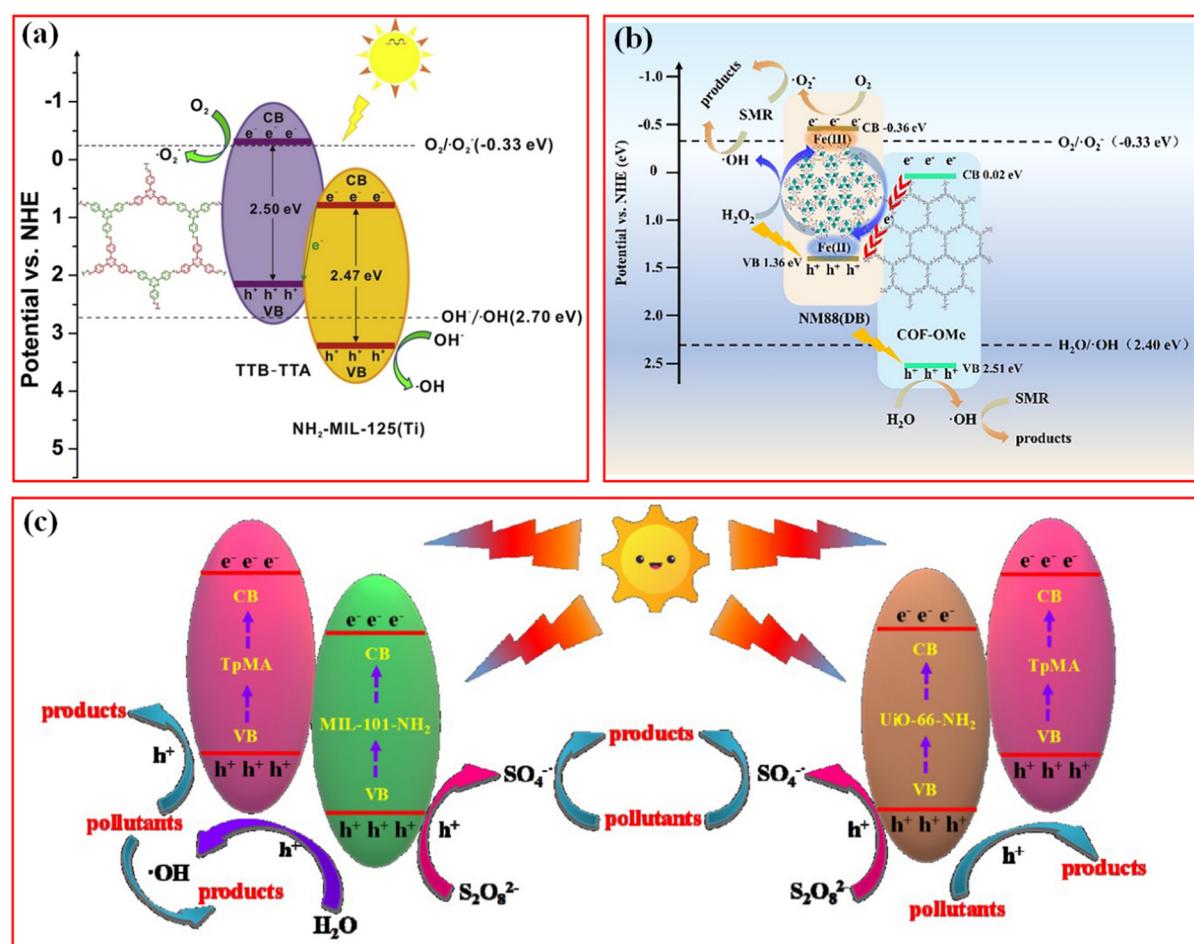
Fig. 11 (a) Z-scheme charge-transfer mechanisms for the NH2-MIL-125(Ti)/TTB-TTA system. Reproduced with permission.[46] Copyright 2019, Elsevier. (b) Proposed mechanism of the photo-Fenton degradation of SMR in the NM88(DB)$_{0.85}$/COF-OMe/H_2O_2/visible light system. Reproduced with permission.[123] Copyright 2022, Elsevier. (c) Schematic diagram for the possible photocatalytic mechanism of BPA degradation over MIL-101-NH2@TpMA and UiO-66-NH2@TpMA under visible light irradiation. Reproduced with permission.[47] Copyright 2020, Elsevier.

(SMR),[123] TTA-BPDA-COF@ZIF-L-Co for RhB and bisphenol A (BPA),[76] and NM-125(Ti)$_x$@TpTta-COF for BPA.[51]

In fact, adding an appropriate amount of H_2O_2 into Fe-based MOFs-containing catalytic reaction system is an effective strategy for improving the yield of $^\bullet$OH, even though the accumulated holes have insufficient oxidizing ability to directly generate $^\bullet$OH from H_2O. The presence of H_2O_2 could accelerated the Fe(III)/Fe(II) cycle by an enhanced electronic effect; in detail, the conversion of Fe(III) to Fe(II) is achieved by the migration of photoinduced electron to metal sites under light irradiation (Fig. 11b).[123] The formed Fe(II) sites could serve as electron donors to activate H_2O_2 to $^\bullet$OH *via* the Fenton-like reaction, while Fe(II) is oxidized to Fe(III) for the next cyclic loop reaction. Significantly, excess H_2O_2 probably cause decreased photocatalytic efficiency, where $^\bullet$OH could react with H_2O_2 to form abundant inactive $^\bullet HO_2$ radicals.[124]

Apart from H_2O_2, peroxymonosulfate (PMS) or peroxydisulfate (PS) could also be employed to produce the desired robust radicals ($^\bullet SO_4{}^-$), which have even demonstrated superior degradation performance with remarkable oxidation ability compared to $^\bullet$OH. Lv *et al.* fabricated a novel MOFs@COFs/PS system for the photocatalytic degradation of BPA, wherein PS was activated by photogenerated holes to form $^\bullet SO_4{}^-$ as dominant radicals (Fig. 11c).[47] The good universal applicability of coupling MOF/COF composites with sulfate radical-based advanced oxidation processes is confirmed by the excellent degradation performance toward other organic pollutants such as methylene blue (MB) and methyl orange (MO). Interestingly, recent studies find that the carbonization of MOF/COF composites not only maintain their inherent metal active sites and structural advantages but also improve the electrical conductivity and even introduce new active sites including oxygen vacancy, surface hydroxyl groups, ketone groups, and graphitic N. Li *et al.* reported a novel nanocomposite catalyst (CC@Co$_3$O$_4$) derived from COF@ZIF-67 for visible light-driven activation of peroxymonosulfate (PMS) to degrade BPA and RhB. Unlike previous research using the MOFs@COFs/PS system, this updated photocatalyst system could be applied in a wider pH range and generate more radical types, especially $^1O_2$, which mainly contributed to the enhanced catalytic degradation performance.[88]

Because of the COVID-19 pandemic, the application of photocatalysis technology into biomedical research has attracted tremendous interest. Similar to the photocatalytic degradation of organic pollutants, photocatalytic filters against pathogenic bioaerosols are also an oxidation process but milder in light of the tolerance of the physical body. The most suitable ROS to eliminate pathogenic microorganisms efficiently and safely is singlet oxygen ($^1O_2$). Li *et al.* designed a core–shell ZIF-8@iCOF nanocomposite, which exhibited ultrahigh $^1O_2$ generation efficiency (2.2 times that of bare COFs) and antibacterial efficiency of 99.99999% after 15 min irradiation.[125] Specifically, cationic iCOF layers served as a light capture antenna to harvest photoinduced electron–hole pairs, and the generated electrons subsequently migrated to the ZIF-8/iCOF heterointerface. Owing to the conjugated periodic

structure in the interface, abundant $^1O_2$ were produced by the efficient transfer of the migrated excitons into a lower-energy triplet excited states (T1) *via* the intersystem crossing (ISC) of iCOF. At the same time, the rapid mass transfer of the porous heterointerface accelerated the intermolecular interactions with O_2 and facilitated the rapid diffusion of generated $^1O_2$. This investigation not only provides an innovative method to design high-performance self-cleaning filter by structural engineering but also encourages researchers to extend the application of MOF/COF-catalyzed photodegradation into more research fields.

4. Thermocatalytic applications of MOF/COF composites

MOFs have been extensively used as traditional heterogeneous catalysts for a variety of reactions because of their large surface area and porosity, abundant unsaturated metal ions, tailorable organic linkers, and metal nodes, with various possibilities to be designed and modified after synthesis.[126,127] However, the thermal catalysis method has the disadvantages of high energy consumption, high requirements of equipment, and high reaction temperature in application, which shortens the life of the catalyst in the catalytic process. The surfaces and pores of some MOFs are hydrophilic, leading to difficulties in the aggregation of hydrophobic substrates. Most of these disadvantages limit their practical applications in multiphase catalysis. To overcome this problem, the modification of MOFs with other functional materials has been achieved, thus combining their advantages and disadvantages to improve the performance.[128] COFs, as an emerging porous crystalline material fully formed by organic molecules through a covalent bonding process, have also attracted extensive research attention in catalysis.[129] Core–shell hybrid MOF/COF composites, such as NH$_2$-MIL-68@TPA-COF and NH$_2$-UiO-66/TpPa-1-COF, have been synthesized and show effectiveness in photocatalytic dye degradation and photocatalytic hydrogen precipitation, respectively. Therefore, novel core–shell MOF/COF are also expected to be used for multiphase catalysis.

4.1 Thermocatalytic selective oxidation

The selective oxidation of organic substrates to value-added chemicals over heterogeneous catalysts is important in the organic synthesis field, and remarkable efforts have been attributed to the research and development of efficient earth-abundant metal-based catalysts.[130] Thanks to the unique structure and properties of MOFs, MOFs-based materials have been investigated as efficient catalysts with outstanding performance in the oxidation of organic substances.[126] However, in most MOF structures, active metal sites surrounded by nonreactive organic linkers may be limited for the binding and activation of the substrates. Moreover, the poor stability of MOFs in some organic solvents usually causes the leaching of the active metal species from MOFs. One of the effective methods is to functionalize the MOFs surface to increase their catalytic activity and

structural stability toward the selective oxidation of organic substances.

For example, to improve the adsorption of hydrophobic organic substrates, Li *et al.* developed hierarchical porous NH$_2$-MIL-101(Fe)@NTU-COF composites using hydrophilic MOF nanocrystal as the core and mesoporous hydrophobic NUT-COF as the shell for the selective oxidation of styrene to benzaldehyde with *tert*-butyl hydroperoxide (TBHP) as the oxidant (Fig. 12a).[21] The NH$_2$-MIL-101(Fe)@NTU composite exhibits considerably improved catalytic conversion and selectivity during styrene oxidation (Fig. 12b).[21] Using nonhomogeneous Lewis acids as catalysts, the free radicals directly attacked the C═C of styrene under the synergistic effect of the COF shell and MOF core to produce benzaldehyde and formaldehyde in the absence of styrene epoxide. In the reaction process, NH$_2$-MIL-101(Fe) provided unsaturated catalytic sites for coordination, and the NTU-COF shell aggregated hydrophobic molecular substrates and promoted the free radical mechanism for the direct formation of benzaldehyde from styrene (Fig. 12c). The conversion (32%) of styrene and selectivity (84%) of benzaldehyde were achieved.[21] This method, based on MOF/COF to synthesize NH$_2$-MIL-101(Fe)@NTU composites, improved the catalytic performance of the catalyst in wet environment.

Even though there have only been few studies on the use of MOF/COF composites in thermocatalytic selective oxidations, the rational design of MOF/COF composites with different hydrophilic and hydrophobic properties would facilitate the adsorption and activation of organic substrates. In addition, for improved catalytic performance, the unsaturated active sites, pore environment, and coordination sites of the catalysts should be carefully regulated by adjusting the substrate molecular diffusion, molecular adsorption, interface reaction, product desorption, and diffusion.

4.2 Thermocatalytic selective reduction

The research on thermocatalytic selective reduction reactions is becoming increasingly popular as the industrial, chemical, and pharmaceutical industries place greater emphasis on the selectivity required for their target products.[130] For thermocatalytic selective reduction reactions, size-selective catalysis

and selective reduction of polar unsaturated groups are the two most researched types. It is crucial that the selectivity is not improved at the expense of the reactivity, but the design of the material should preferably meet the compromise balance of reactivity, selectivity, and stability. The MNPs@MOFs composites have become essential materials for current thermocatalytic selective reduction reactions,[116,131,132] but there are still problems such as metal leaching, hindered active sites, and poor selectivity regulation.

In recent years, the construction of sandwich-structured nanocomposites has provided an excellent strategy for solving challenging size-selective catalytic processes. For example, Tang's research group proposed the use of MOFs as the regulator of selective hydrogenation reaction and subtly designed and precisely constructed sandwich-structured MIL-101@Pt@MIL-101 catalyst.[133] Compared with single Pt nanoparticles and supported catalysts, the sandwich-structured catalyst possesses extremely high selective hydrogenation performance for cinnamaldehyde (selectivity of ∼95.6% and conversion of ∼99.8%). Given that this design concept displays a high universality for enhancing the selectivity, many similar catalytic materials have been developed for the production of high quality chemicals, such as UiO-67@Pd@UiO-X (X = 66, 67, and 68),[134] MIL-88B(Fe)@Pt@Al-TCPP,[135] and ZIF-8x@Pd@ZIF-8.[136] Furthermore, researchers have previously studied that the coating of the MIL-101@Pt surface with hydrophobic conjugated microporous polymer and iron(III) porphyrin (FeP-CMPs) shell can not only effectively change the wettability of the material but also change the environment of Pt NPs and realize the selective hydrogenation of the polar C═O bond in cinnamaldehyde (Fig. 13a).[65] Similarly, COFs also have many advantages such as tunable hydrophobicity, which will show great potential for the effective enrichment of substrate molecules and the regulation of the metal chemical environment. Therefore, COFs have become the preferred shell material for the regulation of selective catalysis due to their ordered porous structure, π-conjugated structure, high specific surface area, high thermal stability, and tunable hydrophobicity. For instance, Zhou *et al.* constructed Pd/UiO-66-NH$_2$@COF materials and studied the effect of mesoporous COF shell layer thickness on the activity and size selectivity of olefin
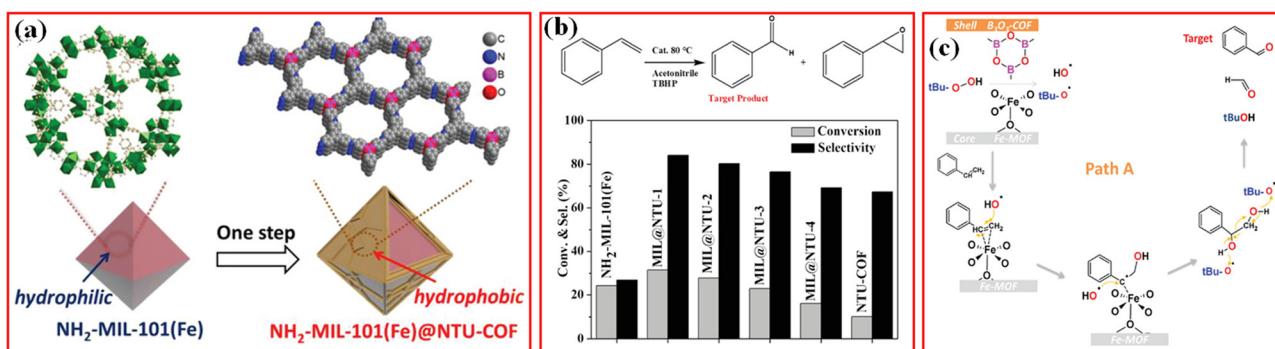

Fig. 12 (a) Fabrication of NH$_2$-MIL-101(Fe)@NTU-COF; (b) Styrene oxidation reaction catalyzed by different catalysts using TBHP as the oxidant; (c) proposed mechanism path A for styrene transformed to benzaldehyde. Reproduced with permission.[21] Copyright 2019, Wiley-VCH.
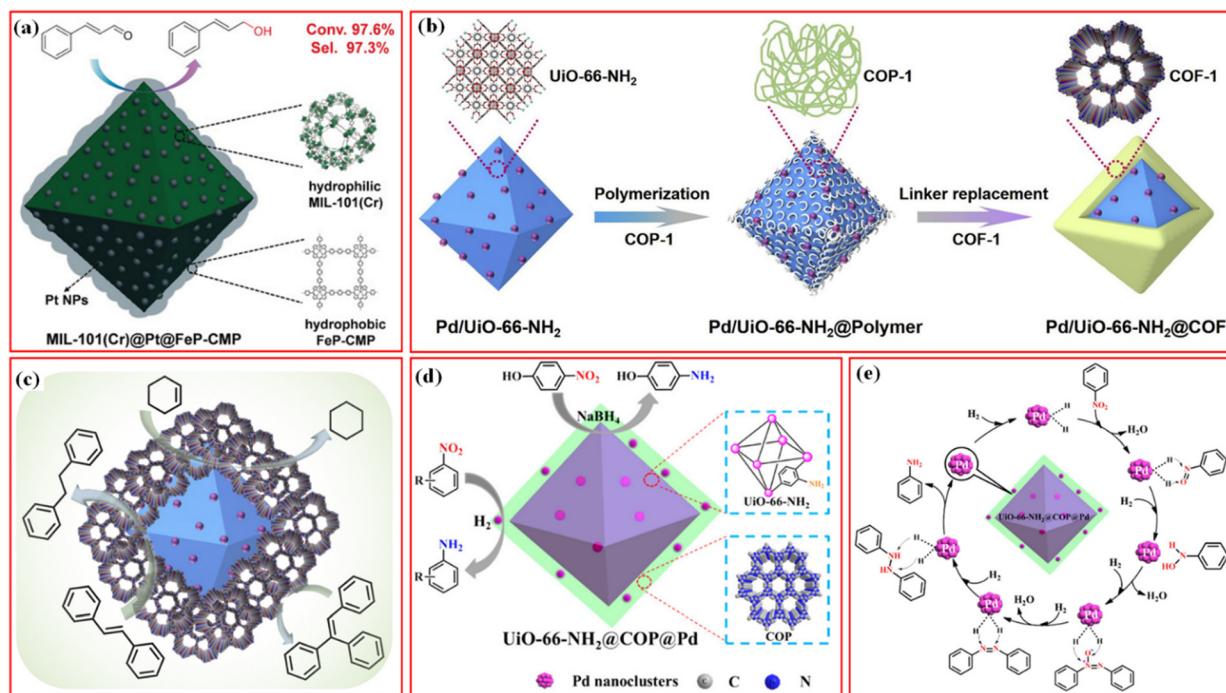
Fig. 13 (a) Illustration of the structure and selective hydrogenation of the polar C=O bond in cinnamaldehyde over MIL-101(Cr)@Pt@FeP-CMP. Reproduced with permission.[65] Copyright 2018, Wiley-VCH. (b) Schematic illustration for the preparation of the sandwiched Pd/UiO-66-NH$_2$@COF composite and (c) selective hydrogenation using the Pd/UiO-66-NH$_2$@COF composite. Reproduced with permission.[68] Copyright 2020, Elsevier. (d) Schematic illustration of the structure and reaction over Pd nanoclusters-doped UiO-66-NH$_2$@COP hybrid material and (e) possible reaction mechanism for the catalytic hydrogenation of nitrobenzene to aniline with UiO-66-NH$_2$@COP@Pd. Reproduced with permission.[70] Copyright 2020, ACS Publishing Group.

hydrogenation reactions (Fig. 13b).[68] Due to the steric hindrance effect and diffusion barrier, the reaction activity usually decreases with the increase in the substrate molecular size, for example, the triphenylethylene molecules larger than the pore size of the COF-1 shell (the mesoporous pore of 2.7 nm) cannot be converted; thus, COF-1 can be used as an effective size selection regulator for catalytic reaction (Fig. 13c).

In addition, the spatial confinement effect of the porous structure of MOF/COF could regulate the location and distribution of MNPs, and the interaction between metals and porous supports is related to the dispersion and stability of metals, which has also become very important features of MOF@COFs-based materials in selective reduction. Zhu *et al.* used inverse double solvent method (RDSA) to encapsulate ultrafine Pd nanoclusters in UiO-66-NH$_2$@COP (Fig. 13d).[70] The uniform distribution of heteroatoms (N) in COPs makes it an ideal platform for anchoring Pd species and restrict the growth of Pd nanoclusters, thus improving the utilization of Pd active sites. Moreover, hybrid materials with micro- and mesopores have higher porosity than single MOFs or COFs, thus contributing to the maximization of contact between reactants and active sites as well as the rapid separation of products (Fig. 13e). Importantly, the stable structure of the COF shell and the metal-support interaction prevented the metal leaching of Pd active sites and showed good cycle stability in the reduction reaction of 4-nitrophenol (4-NP).

Although these characteristics of the shell layer of COFs have seldom been investigated, this should be an interesting direction of research in thermocatalytic selective reduction reactions. Ultimately, hybrid materials comprising MOFs, MNPs, and COFs exhibit promising applications in thermocatalytic reduction reactions due to their unexpected synergistic effects, catalytic active sites, unique confinement environments, size-dependent characteristics, and abundant porosity.

4.3 Other reactions

Besides the applications of MOF/COF composites in thermocatalytic selective oxidation and reduction reactions, MOF/COF composites have also been applied in some other reactions, such as Knoevenagel condensation reaction, CO$_2$ cycloaddition, and C–C coupling reaction.[20,137,138] Knoevenagel condensation reaction, as a nucleophilic addition reaction, has been widely used to construct the C=C group, which can be further used in the construction of medical drugs, polymers, active materials, and other materials of intermediates or products.[139] A macroporous polymer monolith with a ZIF-8 coating covering the pore surface was prepared by Maya *et al.* via a two-step nanoparticle orientation route for the catalytic Knoevenagel condensation reaction of benzaldehyde and ethyl cyanoacetate.[140] The presence of ZIF-8 in the monolith greatly accelerated the reaction, reaching 97% conversion after 110 min, and the catalytic activity remained even after 18 h of

continuous reaction under flow conditions. Han *et al.* prepared a core–shell UiO-66@SNW-1, a bifunctional acid–base catalyst containing both Lewis acid and Brønsted base sites, which showed durable catalytic activity, excellent recoverability, and outstanding stability in the one-pot tandem deacetaldehyde-Knoevenagel condensation reaction.[141]

Recently, Co-MOF/COF and Zn-MOF/COF composites synthesized by Rafiee *et al.* showed good catalytic activity in the Knoevenagel condensation reaction, which was characterized by a short catalytic reaction time and high catalytic yield.[142] Co-MOF/COF was used for the condensation of several aldehydes with malononitrile to produce benzylidene malononitrile derivatives in high yields (62–94%) and short reaction times (5–60 min). Unlike the use of amino-functionalized MOFs to bind imine-linked COFs, Han *et al.* prepared a kind of π–π stacked cobalt-based PCN-222-Co@TpPa-1 for the Knoevenagel condensation reaction.[20] The unsaturated Zr(IV) and Co(II) centers catalyzed the dimethyl acetal of benzaldehyde to produce benzaldehyde, and the imine group in TpPa-1 catalyzed the Knoevenagel condensation reaction to produce 2-benzylidenemalononitrile. The core–shell PCN-222-Co@TpPa-1 exhibited high catalytic activity (99.3% yield) and good recoverability in the one-pot deacetylation-Knoevenagel condensation cascade reaction.[20]

In addition to core–shell materials, yolk–shell (YS) MOF/COF composites have also been used in the Knoevenagel condensation reaction. Dang *et al.* developed a general solvothermal method to fabricate YS-COF@MOF nanocomposites by an efficient template-free strategy.[58] The subsequent condensation reaction yields the core–shell structure polyimine@MOF as a result of the weak interaction between the MOF surface and the monomer. The disordered polyimide reorganized and reconstructed into an ordered framework to form a crystalline shell under solvothermal conditions. During the shrinkage, the shell separates from the MOF core under pyrrolidine-catalyzed conditions, resulting in a gap between the core and the shell, giving rise to YS-COF@MOF. The formed special cavity not only exposed more active sites for the reactants but also provided a special microenvironment for heterogeneous catalysis. As a result, the YS-TpPa@UiO-66-(COOH)$_2$ nanocomposite integrated the inherent structural tunability and functionality of COF and MOF and could effectively catalyze the one-pot tandem D-K condensation reaction of benzaldehyde dimethylacetal and malononitrile with a 99% yield of the benzylidenemalononitrile product. The catalyst was applied at least five more times without noticeably losing the catalytic activity.

Besides the Knoevenagel condensation reaction, MOF/COF composites have also been applied in the cyclization reaction of CO_2 and epoxide to synthesize cyclic carbonates, which has a wide range of applications in fine chemicals because of the high resource utilization efficiency and a wide range of products. The efficiency of single-functional MOF catalysts is poor, and Ma *et al.* proposed a strategy to construct the MOF@iPOF (porous organic framework material) core–shell bifunctional catalysts by integrating CUS-based MOF and ionic POF to form CO_2 cyclization heterogeneous catalysts with ultrahigh activity

under mild conditions (60 °C, 0.5 MPa CO_2, 24 h) without co-catalysts.[137] Han *et al.* further prepared porous MOF@POP (porous organic polymer) core–shell structures (NH$_2$-UiO-66(Hf)@CoTPy-CAP) by introducing NH$_2$-UiO-66(Hf) in the synthesis of CoTPy-CAP.[143] Unlike the above core–shell structure, the formation of core–shell structure of ionic porphyrin-based POPs and MOF in the catalyst system as a bifunctional catalyst for CO_2 cyclization was reported for the first time by Han *et al.* They coated CoTPy-CAP shell on NH$_2$-UiO-66 (Hf) to form a core–shell MOF@POP structure, which not only increased the exposure of active sites in CoTPy-CAP but also increased the exposure of Hf clusters. Using the porphyrin Co(II) of CoTPy-CAP and the Hf cluster of NH$_2$-UiO-66(Hf) as Lewis acid sites, the core–shell structure with the bromine ion as the nucleophilic center can catalyze the CO_2 cyclization reaction efficiently under catalyst-free and mild conditions, and its excellent catalytic activity in five cycles indicates its stability and recoverability. COF combined with MOF has shown excellent performance in the field of CO_2 cyclization, but the core–shell MOF/COF composites are still immature and have some shortcomings in industrial applications. Therefore, the scientific research value of core–shell MOF/COF materials is worth exploring, and it would be a meaningful study to explore their applications in catalysis.

The establishment of C–C bonds is crucial for synthetic organic chemistry and the pharmaceutical industry. Recently, stable MOF@COF hybrids have received increasing attention by grafting COF onto MOF through chemical bonding (–C=N–). The hybrid materials combine the benefits of COF and MOF in addition to structural features. They have been employed in a variety of applications, including materials for catalysis, gas storage, and energy storage. Wu reported the fabrication of a novel MOF@COF hybrid structure through the combination of a COF and an amino-functionalized MOF.[64] The catalyst displayed high catalytic activity for the C–C coupling reaction of pyrimidine sulfonate and arylboronic acid. MOF@COF-Pd exhibited good stability, no metal loss, good recyclability, and could be continuously utilized for five cycles.

The MOF@COF composites have demonstrated their excellent performance and stability in Knoevenagel condensation reactions, CO_2 cyclization reactions, and C–C coupling reactions by increasing the exposure of active sites in the material through the use of π-like structures between MOFs and COFs or coating to form MOF@COF structures. MOF@COF composites can also be used in mobile catalysis and extraction of environmental micropollutants or in other applications such as stationary phases for liquid chromatography and preparation of mobile enzymes.

5. Electrocatalytic applications

Electrocatalysis has been extensively investigated because of its great potential and practical applications in the modern energy storage and conversion field for a sustainable world, such as electrocatalytic water splitting to produce H_2 and O_2, fuel cells

and metal-air batteries to produce electricity, and electrocatalytic synthesis of value-added chemicals.[144–146] Zeolite imidazolate skeletons (ZIFs) are a favorable precursor material for the preparation of electrocatalysts due to their tunable composition, sufficient N content, large specific surface area (SSA), and graded porosity. COFs with precisely tunable porous structure, topology, and active centers have become promising next-generation electrocatalytic materials.[147] Lin *et al.* reported a simple and robust route to obtain double-shell Co, N and S co-doped hollow carbon nanocages (denoted as Co–N/S-DSHCN) with excellent ORR performance. The simultaneous composition and structural engineering of the zeolitic imidazolium salt backbone (ZIF-67), achieved by its trithiocyanuric acid (TCA) coating, yielded core–shell precursor particles that were subsequently carbonized to Co–N/S-DSHCN.[148] Lin *et al.* also prepared hollow porous carbon in cages co-doped with Co and N *via* zeolitic imidazolium salt framework (ZIF)-triggered rapid polymerization of dopamine for efficient ORR and OER electrocatalysts.[149] Even though MOFs and COFs with unique structures and properties have been investigated as efficient electrocatalysts for oxygen evolution reaction (OER), hydrogen evolution reaction (HER), oxygen reduction reaction (ORR), CO_2 reduction reaction (CO_2RR), selective oxidation of organics, *etc.*,[150–153] the MOF/COF composites have been rarely reported as electrocatalysts.

Electrochemical ORR is one of the most important reactions in the field of energy conversion. ORR can proceed *via* two pathways: $2e^-$ ORR to produce H_2O_2 and $4e^-$ ORR to produce H_2O. $4e^-$ ORR can be used in proton exchange membrane fuel cells (PEMFC) and rechargeable metal-air cells. Therefore, the development of low-cost, robust, and highly active catalysts is highly desirable for ORR.[154] So far, carbon-based materials including carbon nanotubes, graphene, and porous carbon have been used to support metal-containing compounds such as oxides, carbides, and nitrides as efficient ORR electrocatalysts.[155] Carbon-based materials not only provide anchor sites for individual metal atoms and good electrical conductivity with graphite-like backbones but also modulate the charge density and electronic structure of metal atoms or nanoparticles. To date, COFs typically exhibit low electrocatalytic activity because of their poor electrical conductivity. MOFs- or COFs-derived materials obtained *via* pyrolysis have been widely exploited as ORR electrocatalysts because of their high surface area, permanent porosity, and varied structure.[156,157] There are also some efforts using MOF/COF-derived materials as ORR electrocatalysts.

Yamauchi *et al.* reported a novel strategy to achieve the controlled integration of β-ketoenamine-linked 2,6-diamino-anthraquinone (DAAQ)-1,3,5-trimethylphenol (TFP)-COF (DAAQ-TFP-COF) with MOF-derived graphitic carbon (GC) to form a well-defined GC@COF core–shell structure, followed by thermal transformation to yield graphitic nitrogen-doped porous carbon (NC), referred to as GC@COF-NC (Fig. 14a).[85] The resulting GC@COF-NC core–shell heterostructure with high electrical conductivity, layered pores (micropores and mesopores), and abundant nitrogen-doped catalytic edges shows
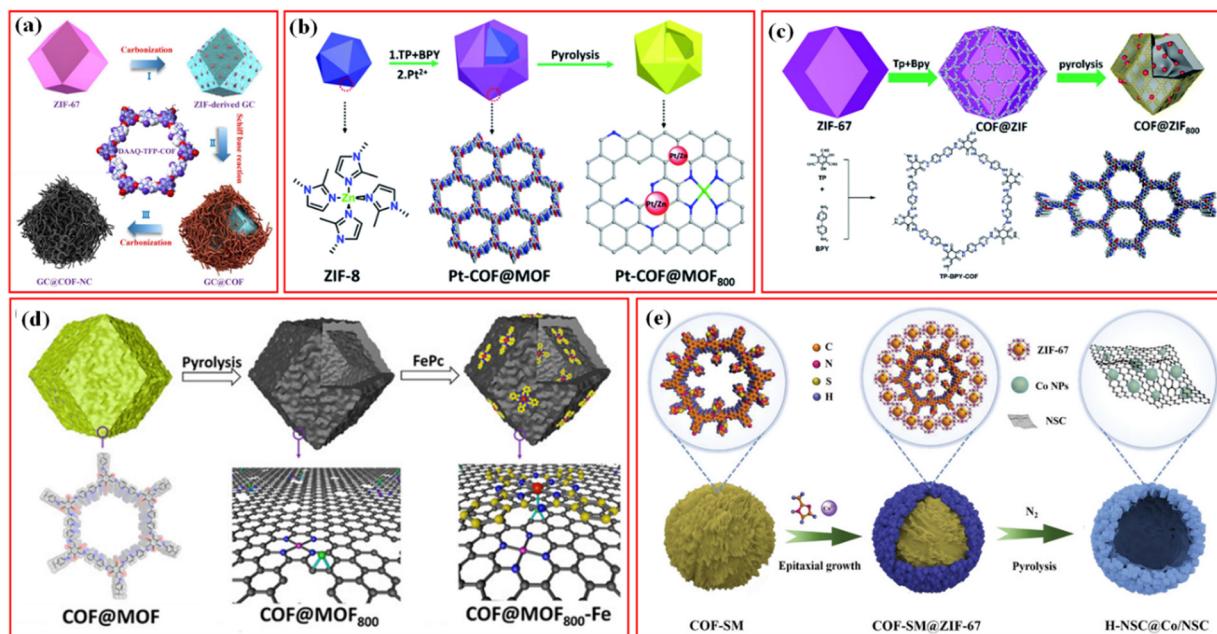
Fig. 14 (a) Schematic illustration of the formation of the GC@COF-NC heterostructure. Reproduced with permission.[85] Copyright 2020, Elsevier. (b) Schematic of the synthesis procedure of the Pt-COF@MOF$_{800}$ catalyst from TP-BPY-COF encapsulated ZIF-8. The red balls in Pt-COF@MOF$_{800}$ represent Pt/Zn bimetal nanoparticles. Reproduced with permission.[24] Copyright 2021, Royal Society of Chemistry. (c) Schematic of COF@MOF$_{800}$-Fe synthesis from COF@MOF (the black, purple, red, green, and blue balls represent carbon, zinc, iron, oxygen, and nitrogen atoms, respectively). Reproduced with permission.[25] Copyright 2022, Royal Society of Chemistry. (d) Schematic of the synthesis procedure of the COF@ZIF$_{800}$ catalyst by *in situ* growing the TP-BPY-COF on the surface of ZIF-67. Reproduced with permission.[89] Copyright 2022, Wiley-VCH. (e) Schematic illustration of the synthesis process of the core–shell H-NSC@Co/NSC hybrid. Reproduced with permission.[26] Copyright 2022, Wiley-VCH.

high ORR electrocatalytic performance, with comparable initial voltage (0.923 V *vs.* RHE) and half-wave potential (0.841 V *vs.* RHE) and higher long-term stability compared to 20 wt% Pt/C commercial catalysts.

For the first time, Zeng *et al.* designed and built a stable and highly active ORR catalyst from a COF@MOF hybrid, in contrast to Yamauchi's work employing carbon generated from MOFs as a template.[24] The COF@MOF-derived layered carbon polyplatinum catalyst (Pt-COF@MOF$_{800}$) was achieved through a multistep process that included the preparation of ZIF-8 nanocrystals, *in situ* encapsulation of ZIF-8 with thin TP-BPY-COF layers from 2,4,6-trihydroxybenzene-1,3,5-trialdehyde (TP) and [2,20-bipyridyl]-5,50-diamine (BPY), introduction of platinum ions into the hybrid COF@MOF, and structural and textural reorganization under controlled pyrolysis at 800 °C for 1 h (Fig. 14b). The introduction of Pt^{2+} promoted the formation of the hollow morphology due to the Kirkendall effect. The MOF core not only acted as a Zn source for atomic Zn and ZnPt nanoparticles but also served as a template for COF growth and prevented COF aggregation during pyrolysis. Finally, Zn atoms from ZIF-8 and sub-3 nm Pt/Zn bimetallic clusters/nanoparticles were immobilized on hollow carbon to create the catalyst. With these features, the catalyst exhibited half-wave potentials of 0.85 and 0.85 V for ORR under alkaline and acidic conditions, respectively, which were higher than those of Pt/C. Following this, Zeng *et al.* further designed and synthesized Co nanoparticles and carbon embedded with Co–N$_4$ atoms by a similar method *via* the direct pyrolysis of TP-BPY-COF@ZIF-67 using ZIF-67 crystals as the core for catalytic ORR and HER (Fig. 14c).[25] The resulting COF@ZIF$_{800}$ exhibited bifunctional catalytic performance for ORR and HER, where the half-wave potential for ORR in 0.1 M KOH was 0.85 V and the overpotential for HER in 1 M KOH at 10 mA cm^{-2} was 0.16 V. In addition to the preparation of electrocatalysts with bifunctionality, Zeng *et al.* fabricated hollow carbon (COF@-MOF$_{800}$) by the pyrolysis of COF@MOF at 800 °C for 1 h, which contained a high content of atomic Zn and plentiful N and O groups (Fig. 14d).[89] Afterward, a second atomic metal Fe was introduced to form biphasic atomic Zn–N$_4$ and Fe–N$_4$O catalysts, resulting in COF@MOF$_{800}$-Fe by introducing iron phthalocyanine (FePc). Due to the formation of dual sites (FeN$_4$O and ZnN$_4$) in the carbon, the Fe and Zn sites showed better activity for ORR because of the lower energy barrier for the rate-determining step in ORR, delivering 0.89 V half-wave potential in 0.1 M KOH, which is 50 mV higher than that of Pt/C.

The hybridization of COFs and MOFs is anticipated to successfully produce optimal bifunctional electrocatalysts with ORR and OER activities since it is motivated by the distinctive structures and complimentary advantages of COFs and MOFs. Huang *et al.* proposed a novel approach to fabricate core–shell carbon-based hybrids as efficient bifunctional electrocatalysts for ORR and OER by the pyrolysis of covalently-linked COF@MOF hybrids, which were synthesized by the epitaxial growth of ZIF-67 nanospheres on imidazole-functionalized COF (COF-SM) (Fig. 14e).[26] The hybrid has a unique core–shell structure, H-NSC@Co/NSC, containing a core of hollow N,S co-doped

carbon derived from COF (H-NSC) and a shell of Co nanoparticles (NPs) embedded in a carbon base derived from ZIF-67 (Co/NSC). Due to the unique hollow structure and the strong synergistic effect between the carbon matrix and the embedded Co NPs, the resulting core–shell H-NSC@Co/NSC hybrid demonstrated excellent bifunctional electrocatalytic activity with a small potential gap ($\Delta E = 0.75$ V), which was superior to the most existing reported bifunctional catalysts.

To date, only several electrocatalysts derived from MOF/COF composites have been tried as ORR electrocatalysts even though some also have certain performance in HER or OER. In the future, more work should be done in the investigation of MOF/COF composites as efficient electrocatalysts based on the results of pristine MOFs or COFs electrocatalysts even though their stability in acid and alkaline electrolytes is still a tricky issue. In addition, the structure reconstruction and actual active sites of MOF/COF composites during the electrochemical process should be carefully detected by advanced *in situ* or operando techniques.[158]

6. Conclusion

As two new crystalline porous materials in functional materials, MOF and COF have developed rapidly in recent years; however, due to some inherent flaws, a single MOF or COF cannot meet the specific needs of specific application. The construction of composite materials based on MOFs and COFs has thus been a focus of research to increase the potential uses of the majority of MOFs and COFs. The integration of different components is not only a simple combination of functionality but can also lead to unexpected new features.

Over the past two decades, with the rapid growth of this research field, MOF/COF-based materials have achieved great success in combining the properties and advantages of both homogeneous and heterogeneous catalysts. However, COFs are more difficult to synthesize than other porous materials; thus, Hyunsoo Park's team developed a computational screening algorithm that theoretically achieved heteroepitaxial growth of 3D COFs using a bottom-up approach to create 3D COFs with MOFs as a substrate.[159] Hyunsoo Park *et al.* created 3D COFs through lattice matching and analyzing the interfaces on chemical bonds to build the database. The final screening algorithm determined the MOF@COFs and concluded that selecting COFs with high crystallinity would facilitate the synthesis process.

We thoroughly examine the most recent developments in MOF/COF composites with MOF and COF properties in this review. Initial progress has been made in the preparation and application of MOFs–COFs composites due to the combination of two excellent crystal frameworks. In this review, the preparation of these two composites is described in detail in the following directions: (1) COFs grown on pre-synthesized MOFs; (2) MOFs grown on pre-synthesized COFs. MOF/COF composites constructed by establishing heterojunctions, functionalization, integration, and doping with metal particles are

connected by covalent and noncovalent bonds and thus exhibit higher performance in the field of catalysis. This review summarizes the recent progress of MOF/COF composites in photocatalysis (photocatalytic hydrogen production, photocatalytic selective reduction, photocatalytic selective oxidation, and photocatalytic degradation), thermocatalysis (thermocatalytic oxidation and thermocatalytic reduction), and electrocatalysis. Different ways to make MOF/COF-based catalysts are reviewed in each chapter, and the reaction mechanisms are described in relation to the reaction substrates and the active sites of MOF/COF.

The application and development of MOF/COF composites in the field of catalysis can effectively reduce environmental pollution and resource shortage. However, their research is still in the initial stage. Some products can only be prepared in the laboratory for the time being and are still some distance away from mass production and application. Therefore, further research on the formation mechanism of MOF/COF composites and their reaction mechanism in the catalytic process as well as the extension of their practical applications is the main direction of current research. Specifically, it is shown in the following three aspects.

(1) MOF/COF composites have undergone comparatively less research and design compared to single MOFs and COFs. It is necessary to further develop a deep understanding of the relationship between the structure and functionality of MOF- and COF-based catalysts. The advancement of synthetic strategies has allowed for the design and synthesis of MOF/COF-based catalysts with high porosity and controlled structural orientation, which may function very well in photocatalysis, thermal catalysis, and electrocatalysis.

(2) The mechanism of MOF/COF composites has not been studied deeply enough. Clarifying the structural characteristics and reaction mechanisms of MOFs-based catalysts that influences the catalytic activity of organic conversions under actual reaction conditions could aid researchers in creating catalysts that are more effective for particular catalytic processes. The actual structural changes of MOF/COF catalysts under real reaction circumstances, however, are not well recognized due to the various composition of MOFs-based catalysts, making it difficult to sort out and comprehend their conformational relationships. Advanced *in situ* characterization techniques and theoretical calculations were used to simultaneously examine the reaction intermediates during the actual reactions to better understand the relationship between the structures of MOF/COF catalysts and the corresponding catalytic performance, offering some insights into the reaction mechanisms and catalyst evolution.

(3) The characterization of the properties and structures of MOF/COF composites is not comprehensive enough. Due to the difficulty in exposing Lewis sites and unsuitable pore environments, many MOF/COF require harsh organic reaction conditions, which limits their practical applications. Therefore, MOF/COF catalysts have not received much attention as an efficient catalyst in industry and lack successful applications in industrial processes. In contrast, metal oxide catalysts, which are widely used in industry, are easy to prepare and have a mature technology. To satisfy the industrial need, it is necessary to produce MOFs and COFs with inexpensive precursor structures. The base for the practical application of MOF/COF will be provided by improvements in chemical synthesis techniques, process standardization, and the popularity of smart manufacturing in plants.

Their practical applications should be carefully considered in future research work. For applications, the unique layered porous structure of MOF/COF composites gives them a strong advantage in many fields, but this is to the detriment of their own stability and electrical conductivity. The unsatisfactory stability and poor electrical conductivity are key bottlenecks in the development of MOF-/COF-based catalysts. Therefore, it is important to develop MOFs/COFs with high stability and high conductivity while maintaining their unique structures. In practical applications, the remarkable development of new characterization methods, such as X-ray absorption spectroscopy (XAS) and atomic force microscopy (AFM), should also be considered to reveal more details of MOF/COF as catalysts, which is important for understanding the transition state and catalyst surface interface reactions in the catalytic process and rational design of MOF/COF-based catalysts to obtain better catalytic performance. This is crucial for comprehending the catalytic process and catalyst surface interface reactions as well as for the thoughtful design of MOF/COF-based catalysts with improved catalytic performance. We can foresee that through the unremitting efforts of researchers, MOF/COF-based catalysts will surpass traditional homogeneous or multiphase catalysts in terms of activity and selectivity in the future.

Conflicts of interest

There are no conflicts to declare.

Acknowledgements

Notes and references

1 G. Chakraborty, I.-H. Park, R. Medishetty and J. J. Vittal, Two-dimensional Metal–Organic Framework materials: Synthesis, structures, properties and applications, *Chem. Rev.*, 2021, **121**, 3751–3891.

2 O. M. Yaghi, G. Li and H. Li, Selective binding and removal of guests in a microporous metal–organic framework, *Nature*, 1995, **378**, 703–706.

3 G.-B. Wang, K.-H. Xie, H.-P. Xu, Y.-J. Wang, F. Zhao, Y. Geng and Y.-B. Dong, Covalent organic frameworks and their composites as multifunctional photocatalysts for efficient visible-light induced organic transformations, *Coord. Chem. Rev.*, 2022, **472**, 214774.

4 Y. Zhang, H. Liu, F. Gao, X. Tan, Y. Cai, B. Hu, Q. Huang, M. Fang and X. Wang, Application of MOFs and COFs for photocatalysis in CO2 reduction, H2 generation, and environmental treatment, *EnergyChem*, 2022, **4**, 100078.

5 Y. Chen, W. Li, X.-H. Wang, R.-Z. Gao, A.-N. Tang and D.-M. Kong, Green synthesis of covalent organic frameworks based on reaction media, *Mater. Chem. Front.*, 2021, **5**, 1253–1267.

6 S. M. Moosavi, A. Nandy, K. M. Jablonka, D. Ongari, J. P. Janet, P. G. Boyd, Y. Lee, B. Smit and H. J. Kulik, Understanding the diversity of the metal–organic framework ecosystem, *Nat. Commun.*, 2020, **11**, 4068.

7 R. Anderson and D. A. Gómez-Gualdrón, Increasing topological diversity during computational ''synthesis'' of porous crystals: how and why, *CrystEngComm*, 2019, **21**, 1653–1665.

8 M. Ma, X. Lu, Y. Guo, L. Wang and X. Liang, Combination of metal–organic frameworks (MOFs) and covalent organic frameworks (COFs): Recent advances in synthesis and analytical applications of MOF/COF composites, *TrAC-Trend Anal. Chem.*, 2022, **157**, 116741.

9 Y. Li, M. Karimi, Y.-N. Gong, N. Dai, V. Safarifard and H.-L. Jiang, Integration of metal–organic frameworks and covalent organic frameworks: Design, synthesis, and applications, *Matter*, 2021, **4**, 2230–2265.

10 M. Chen, H. Li, C. Liu, J. Liu, Y. Feng, A. G. H. Wee and B. Zhang, Porphyrin- and porphyrinoid-based covalent organic frameworks (COFs): From design, synthesis to applications, *Coord. Chem. Rev.*, 2021, **435**, 213778.

11 C. Gong, X. Yang, X. Wei, F. Dai, T. Zhang, D. Wang, M. Li, J. Jia, Y. She, G. Xu and Y. Peng, Three-dimensional porphyrin-based covalent organic frameworks with stp topology for an efficient electrocatalytic oxygen evolution reaction, *Mater. Chem. Front.*, 2023, **7**, 230–237.

12 Y. Deng, Y. Wang, X. Xiao, B. J. Saucedo, Z. Zhu, M. Xie, X. Xu, K. Yao, Y. Zhai, Z. Zhang and J. Chen, Progress in hybridization of Covalent Organic Frameworks and Metal–Organic Frameworks, *Small*, 2022, **18**, 2202928.

13 L. Garzón-Tovar, J. Pérez-Carvajal, A. Yazdi, J. Hernández-Muñoz, P. Tarazona, I. Imaz, F. Zamora and D. Maspoch, A MOF@COF composite with enhanced uptake through interfacial pore generation, *Angew. Chem., Int. Ed.*, 2019, **58**, 9512–9516.

14 M. L. Yola and N. Atar, Amperometric galectin-3 immunosensor-based gold nanoparticle-functionalized graphitic carbon nitride nanosheets and core–shell Ti-MOF@COFs composites, *Nanoscale*, 2020, **12**, 19824–19832.

15 L. Zhang, Z. Liu, Q. Deng, Y. Sang, K. Dong, J. Ren and X. Qu, Nature-inspired construction of MOF@COF nanozyme with active sites in tailored microenvironment and pseudopodia-like surface for enhanced bacterial inhibition, *Angew. Chem., Int. Ed.*, 2021, **60**, 3469–3474.

16 Y. Chen, D. Yang, B. Shi, W. Dai, H. Ren, K. An, Z. Zhou, Z. Zhao, W. Wang and Z. Jiang, In situ construction of hydrazone-linked COF-based core–shell heteroframeworks for enhanced photocatalytic hydrogen evolution, *J. Mater. Chem. A*, 2020, **8**, 7724–7732.

17 A. P. Côté, A. I. Benin, N. W. Ockwig, M. O'Keeffe, A. J. Matzger and O. M. Yaghi, Porous, Crystalline, Covalent Organic Frameworks, *Science*, 2005, **310**, 1166–1170.

18 Y. Peng, M. Zhao, B. Chen, Z. Zhang, Y. Huang, F. Dai, Z. Lai, X. Cui, C. Tan and H. Zhang, Hybridization of MOFs and COFs: A new strategy for construction of MOF@COF core–shell hybrid materials, *Adv. Mater.*, 2018, **30**, 1705454.

19 F. Li, D. Wang, Q.-J. Xing, G. Zhou, S.-S. Liu, Y. Li, L.-L. Zheng, P. Ye and J.-P. Zou, Design and syntheses of MOF/COF hybrid materials *via* postsynthetic covalent modification: An efficient strategy to boost the visible-light-driven photocatalytic performance, *Appl. Catal., B*, 2019, **243**, 621–628.

20 M.-L. Gao, M.-H. Qi, L. Liu and Z.-B. Han, An exceptionally stable core–shell MOF/COF bifunctional catalyst for a highly efficient cascade deacetalization–Knoevenagel condensation reaction, *Chem. Commun.*, 2019, **55**, 6377–6380.

21 M. Cai, Y. Li, Q. Liu, Z. Xue, H. Wang, Y. Fan, K. Zhu, Z. Ke, C.-Y. Su and G. Li, One-step construction of hydrophobic MOFs@COFs core–shell composites for heterogeneous selective catalysis, *Adv. Sci.*, 2019, **6**, 1802365.

22 K. Xue, R. He, T. Yang, J. Wang, R. Sun, L. Wang, X. Yu, U. Omeoga, S. Pi, T. Yang and W. Wang, MOF-based In2S3-X2S3 (X = Bi; Sb)@TFPT-COFs hybrid materials for enhanced photocatalytic performance under visible light, *Appl. Surf. Sci.*, 2019, **493**, 41–54.

23 G. Lu, X. Huang, Y. Li, G. Zhao, G. Pang and G. Wang, Covalently integrated core–shell MOF@COF hybrids as efficient visible-light-driven photocatalysts for selective oxidation of alcohols, *J. Energy Chem.*, 2020, **43**, 8–15.

24 Y. Guo, S. Yang, Q. Xu, P. Wu, Z. Jiang and G. Zeng, Hierarchical confinement of PtZn alloy nanoparticles and single-dispersed Zn atoms on COF@MOF-derived carbon towards efficient oxygen reduction reaction, *J. Mater. Chem. A*, 2021, **9**, 13625–13630.

25 M. Liu, Q. Xu, Q. Miao, S. Yang, P. Wu, G. Liu, J. He, C. Yu and G. Zeng, Atomic Co–N4 and Co nanoparticles confined in COF@ZIF-67 derived core–shell carbon frameworks: bifunctional non-precious metal catalysts toward the ORR and HER, *J. Mater. Chem. A*, 2022, **10**, 228–233.

26 W. Li, J. Wang, J. Chen, K. Chen, Z. Wen and A. Huang, Core–shell carbon-based bifunctional electrocatalysts derived from COF@MOF hybrid for advanced rechargeable Zn–air batteries, *Small*, 2022, **18**, 2202018.

27 Z. Wu, W. Li, L. Hou, Q. Wei, H. Yang, Y. Jiang and D. Tang, A novel Sunflower-like MOF@COF for improved

photocatalytic CO2 reduction, *Sep. Purif. Technol.*, 2023, **311**, 123322.

28 Y. Li, X. Song, G. Zhang, L. Wang, Y. Liu, W. Chen and L. Chen, 2D Covalent Organic Frameworks toward efficient photocatalytic hydrogen evolution, *ChemSusChem*, 2022, **15**, e202200901.

29 Z. Li, J. Guo, Y. Wan, Y. Qin and M. Zhao, Combining metal–organic frameworks (MOFs) and covalent-organic frameworks (COFs): Emerging opportunities for new materials and applications, *Nano Res.*, 2022, **15**, 3514–3532.

30 R. Xue, H. Guo, W. Yang, S.-L. Huang and G.-Y. Yang, Cooperation between covalent organic frameworks (COFs) and metal organic frameworks (MOFs): application of COFs-MOFs hybrids, *Adv. Compos. Hybrid Mater.*, 2022, **5**, 1595–1611.

31 C. Guo, F. Duan, S. Zhang, L. He, M. Wang, J. Chen, J. Zhang, Q. Jia, Z. Zhang and M. Du, Heterostructured hybrids of metal–organic frameworks (MOFs) and covalent–organic frameworks (COFs), *J. Mater. Chem. A*, 2022, **10**, 475–507.

32 Z. Chen, X. Li, C. Yang, K. Cheng, T. Tan, Y. Lv and Y. Liu, Hybrid porous crystalline materials from Metal Organic Frameworks and Covalent Organic Frameworks, *Adv. Sci.*, 2021, **8**, 2101883.

33 C. Altintas, I. Erucar and S. Keskin, MOF/COF hybrids as next generation materials for energy and biomedical applications, *CrystEngComm*, 2022, **24**, 7360–7371.

34 G. Yuan, L. Tan, P. Wang, Y. Wang, C. Wang, H. Yan and Y.-Y. Wang, MOF-COF composite photocatalysts: Design, synthesis, and mechanism, *Crystal Growth Des.*, 2022, **22**, 893–908.

35 B. Cui and G. Fu, Process of metal–organic framework (MOF)/covalent–organic framework (COF) hybrids-based derivatives and their applications on energy transfer and storage, *Nanoscale*, 2022, **14**, 1679–1699.

36 M.-X. Wu, Y. Wang, G. Zhou and X. Liu, Sparks from different worlds: Collaboration of MOFs and COFs, *Coord. Chem. Rev.*, 2021, **430**, 213735.

37 M.-Y. Zhang, J.-K. Li, R. Wang, S.-N. Zhao, S.-Q. Zang and T. C. W. Mak, Construction of core–shell MOF@COF hybrids with controllable morphology adjustment of COF shell as a novel platform for photocatalytic cascade reactions, *Adv. Sci.*, 2021, **8**, 2101884.

38 Y. Wan, H. Yang, Q. Shang, Q. Cheng, H. Zhou and Z. Pan, Integrating hollow spherical covalent organic frameworks on NH2–MIL-101(Fe) as high performance heterogeneous photocatalysts, *Environ. Sci.: Nano*, 2022, **9**, 3081–3093.

39 Y. Cheng, Y. Ying, L. Zhai, G. Liu, J. Dong, Y. Wang, M. P. Christopher, S. Long, Y. Wang and D. Zhao, Mixed matrix membranes containing MOF@COF hybrid fillers for efficient CO2/CH4 separation, *J. Membrane Sci.*, 2019, **573**, 97–106.

40 W.-T. Li, Z.-J. Hu, J. Meng, X. Zhang, W. Gao, M.-L. Chen and J.-H. Wang, Zn-based metal organic framework-covalent organic framework composites for trace lead extraction and fluorescence detection of TNP, *J. Hazard. Mater.*, 2021, **411**, 125021.

41 J. Zhao, B. Jin and R. Peng, New core–shell hybrid material IR-MOF3@COF-LZU1 for highly efficient visible-light photocatalyst degrading nitroaromatic explosives, *Langmuir*, 2020, **36**, 5665–5670.

42 H. Peng, J. Raya, F. Richard, W. Baaziz, O. Ersen, A. Ciesielski and P. Samorì, Synthesis of robust MOFs@COFs porous hybrid materials via an aza-Diels–Alder reaction: Towards high-performance supercapacitor materials, *Angew. Chem., Int. Ed.*, 2020, **59**, 19602–19609.

43 J. Wang, L. Wang, D. Zhang, Y. Wang, J. Li, F. Zhou, J. Huang and Y.-N. Liu, Covalently connected core–shell NH2-MIL-125@COFs-OH hybrid materials for visible-light-driven CO2 reduction, *J. Colloid Interface Sci.*, 2023, **637**, 1–9.

44 J. Wang, L. Wang, Y. Wang, F. Yang, J. Li, X. Guan, J. Zong, F. Zhou, J. Huang and Y.-N. Liu, Covalently connected core–shell NH2-UiO-66@Br-COFs hybrid materials for CO2 capture and I2 vapor adsorption, *Chem. Eng. J.*, 2022, **438**, 135555.

45 F.-M. Zhang, J.-L. Sheng, Z.-D. Yang, X.-J. Sun, H.-L. Tang, M. Lu, H. Dong, F.-C. Shen, J. Liu and Y.-Q. Lan, Rational design of MOF/COF hybrid materials for photocatalytic H2 evolution in the presence of sacrificial electron donors, *Angew. Chem., Int. Ed.*, 2018, **57**, 12106–12110.

46 S. He, Q. Rong, H. Niu and Y. Cai, Platform for molecular-material dual regulation: A direct Z-scheme MOF/COF heterojunction with enhanced visible-light photocatalytic activity, *Appl. Catal., B*, 2019, **247**, 49–56.

47 S.-W. Lv, J.-M. Liu, C.-Y. Li, N. Zhao, Z.-H. Wang and S. Wang, Two novel MOFs@COFs hybrid-based photocatalytic platforms coupling with sulfate radical-involved advanced oxidation processes for enhanced degradation of bisphenol A, *Chemosphere*, 2020, **243**, 125378.

48 Y. Wang, Q. Yang, F. Yi, R. Lu, Y. Chen, C. Liu, X. Li, C. Wang and H. Yan, NH2-UiO-66 coated with two-dimensional Covalent Organic Frameworks: High stability and photocatalytic activity, *ACS Appl. Mater. Interfaces*, 2021, **13**, 29916–29925.

49 L. Wang, J. Mao, G. Huang, Y. Zhang, J. Huang, H. She, C. Liu, H. Liu and Q. Wang, Configuration of heteroframework via integrating MOF and triazine-containing COF for charge-transfer promotion in photocatalytic CO2 reduction, *Chem. Eng. J.*, 2022, **446**, 137011.

50 C.-X. Chen, Y.-Y. Xiong, X. Zhong, P. C. Lan, Z.-W. Wei, H. Pan, P.-Y. Su, Y. Song, Y.-F. Chen, A. Nafady, Sirajuddin and S. Ma, Enhancing photocatalytic hydrogen production via the construction of robust multivariate Ti-MOF/COF composites, *Angew. Chem., Int. Ed.*, 2022, **61**, e202114071.

51 L. Yang, Y. Wang, J. Yuan, G. Wang, Q. Cao, H. Fei, M. Li, J. Shao, H. Li and J. Lu, Construction of covalent-integrated MOFs@COFs composite material for efficient synergistic adsorption and degradation of pollutants, *Chem. Eng. J.*, 2022, **446**, 137095.

52 H.-Y. Zhang, Y. Yang, C.-C. Li, H.-L. Tang, F.-M. Zhang, G.-L. Zhang and H. Yan, A new strategy for constructing

covalently connected MOF@COF core–shell heterostructures for enhanced photocatalytic hydrogen evolution, *J. Mater. Chem. A*, 2021, **9**, 16743–16750.

53 W. Han, L.-H. Shao, X.-J. Sun, Y.-H. Liu, F.-M. Zhang, Y. Wang, P.-Y. Dong and G.-L. Zhang, Constructing Cu ion sites in MOF/COF heterostructure for noble-metal-free photoredox catalysis, *Appl. Catal., B*, 2022, **317**, 121710.

54 J. Wang, Z. Dai, L. Wang, D. Zhang, Y. Wang, J. Li, F. Zhou and J. Huang, A Z-scheme heterojunction of porphyrin-based core–shell Zr-MOF@Pro-COF-Br hybrid materials for efficient visible-light-driven CO2 reduction, *J. Mater. Chem. A*, 2023, **11**, 2023–2030.

55 X.-Y. Wang, H.-Q. Yin and X.-B. Yin, MOF@COFs with strong multiemission for differentiation and ratiometric fluorescence detection, *ACS Appl. Mater. Interfaces*, 2020, **12**, 20973–20981.

56 M. Firoozi, Z. Rafiee and K. Dashtian, New MOF/COF hybrid as a robust adsorbent for simultaneous removal of auramine O and rhodamine B dyes, *ACS Omega*, 2020, **5**, 9420–9428.

57 M. Zhang, J.-N. Chang, Y. Chen, M. Lu, T.-Y. Yu, C. Jiang, S.-L. Li, Y.-P. Cai and Y.-Q. Lan, Controllable synthesis of COFs-based multicomponent nanocomposites from core–shell to yolk–shell and hollow-sphere structure for artificial photosynthesis, *Adv. Mater.*, 2021, **33**, 2105002.

58 Q. Dang, H. Huang, L. Li, X. Lyu, S. Zhong, Y. Yu and D. Xu, Yolk–shell-structured Covalent Organic Frameworks with encapsulated Metal–Organic Frameworks for synergistic catalysis, *Chem. Mater.*, 2021, **33**, 5690–5699.

59 W.-T. Li, W. Shi, Z.-J. Hu, T. Yang, M.-L. Chen, B. Zhao and J.-H. Wang, Fabrication of magnetic Fe3O4@metal organic framework@covalent organic framework composite and its selective separation of trace copper, *Appl. Surf. Sci.*, 2020, **530**, 147254.

60 Z. Chen, Z. He, X. Luo, F. Wu, S. Tang and J. Zhang, Synthesis of MOF@COF hybrid magnetic adsorbent for microextraction of sulfonamides in food and environmental samples, *Food Anal. Methods*, 2020, **13**, 1346–1356.

61 M. Zheng, C. Yao and Y. Xu, Fe3O4 nanoparticles decorated with UIO-66 Metal–Organic Framework particles and encapsulated in a triazine-based Covalent Organic Framework matrix for photodegradation of anionic dyes, *ACS Appl. Nano Mater.*, 2020, **3**, 11307–11314.

62 Q. Wang, Y. Zhao, Z. Shi, X. Sun, T. Bu, C. Zhang, Z. Mao, X. Li and L. Wang, Magnetic amino-functionalized-MOF (M = Fe, Ti, Zr)@COFs with superior biocompatibility: Performance and mechanism on adsorption of azo dyes in soft drinks, *Chem. Eng. J.*, 2021, **420**, 129955.

63 K. Zhang, Z. Xi, Z. Wu, G. Lu and X. Huang, Visible-light-induced selective oxidation of amines into imines over UiO-66-NH2@Au@COF core–shell photocatalysts, *ACS Sustainable Chem. Eng.*, 2021, **9**, 12623–12633.

64 Q. Yang, Y. Zhang, N. Ding, Q. Hu, X. Yan, J. Liu, P. Zhang, S. Fu, Q. Wang, L. Wu and S. Wu, A stable MOF@COF-Pd catalyst for C–C coupling reaction of pyrimidine sulfonate and arylboronic acid, *Appl. Organometal. Chem.*, 2022, **36**, e6775.

65 K. Yuan, T. Song, D. Wang, X. Zhang, X. Gao, Y. Zou, H. Dong, Z. Tang and W. Hu, Effective and selective catalysts for cinnamaldehyde hydrogenation: Hydrophobic hybrids of Metal–Organic Frameworks, metal nanoparticles, and micro- and mesoporous polymers, *Angew. Chem., Int. Ed.*, 2018, **57**, 5708–5713.

66 D. Sun and D.-P. Kim, Hydrophobic MOFs@metal nanoparticles@COFs for interfacially confined photocatalysis with high efficiency, *ACS Appl. Mater. Interfaces*, 2020, **12**, 20589–20595.

67 X. Li, K. Zhang, X. Huang, Z. Wu, D. Zhao and G. Wang, Thermo-enhanced photocatalytic oxidation of amines to imines over MIL-125-NH2@Ag@COF hybrids under visible light, *Nanoscale*, 2021, **13**, 19671–19681.

68 W. Zhou, Y. Liu, W. L. Teo, B. Chen, F. Jin, L. Zhang, Y. Zeng and Y. Zhao, Construction of a sandwiched MOF@COF composite as a size-selective catalyst, *Cell Rep. Phys. Sci.*, 2020, **1**, 100272.

69 D. Sun, S. Jang, S.-J. Yim, L. Ye and D.-P. Kim, Metal doped core–shell Metal–Organic Frameworks@Covalent Organic Frameworks (MOFs@COFs) hybrids as a novel photocatalytic platform, *Adv. Funct. Mater.*, 2018, **28**, 1707110.

70 Y. Zhu, W. D. Wang, X. Sun, M. Fan, X. Hu and Z. Dong, Palladium nanoclusters confined in MOF@COP as a novel nanoreactor for catalytic hydrogenation, *ACS Appl. Mater. Interfaces*, 2020, **12**, 7285–7294.

71 J. Fu, S. Das, G. Xing, T. Ben, V. Valtchev and S. Qiu, Fabrication of COF-MOF composite membranes and their highly selective separation of H$_2$/CO$_2$, *J. Am. Chem. Soc.*, 2016, **138**, 7673–7680.

72 N. Zhou, Y. Ma, B. Hu, L. He, S. Wang, Z. Zhang and S. Lu, Construction of Ce-MOF@COF hybrid nanostructure: Label-free aptasensor for the ultrasensitive detection of oxytetracycline residues in aqueous solution environments, *Biosens. Bioelectron.*, 2019, **127**, 92–100.

73 P. Xue, X. Pan, J. Huang, Y. Gao, W. Guo, J. Li, M. Tang and Z. Wang, In situ fabrication of porous MOF/COF hybrid photocatalysts for visible-light-driven hydrogen evolution, *ACS Appl. Mater. Interfaces*, 2021, **13**, 59915–59924.

74 L.-H. Shao, A.-X. Huang, X.-C. Yan, Y.-H. Liu, Y. Wang, X. Jin and F.-M. Zhang, Constructing tightly integrated conductive metal–organic framework/covalent triazine framework heterostructure by coordination bonds for photocatalytic hydrogen evolution, *J. Colloid Interface Sci.*, 2023, **633**, 233–242.

75 H. Fan, M. Peng, I. Strauss, A. Mundstock, H. Meng and J. Caro, MOF-in-COF molecular sieving membrane for selective hydrogen separation, *Nat. Commun.*, 2021, **12**, 38.

76 Y. Deng, Y. Wang, Z. Di, M. Xie, F. Dai, S. Zhan and Z. Zhang, Confining Metal–Organic Framework in the pore of Covalent Organic Framework: A microscale Z-scheme system for boosting photocatalytic performance, *Small Methods*, 2022, **6**, 2200265.

77 Y. Pu, M. Zhao, X. Liang, S. Wang, H. Wang, Z. Zhu, Y. Ren, Z. Zhang, G. He, D. Zhao and Z. Jiang, Growing ZIF-8 seeds on charged COF substrates toward efficient propylene-propane separation membranes, *Angew. Chem., Int. Ed.*, 2023, **62**, e202302355.

78 Q. Niu, S. Dong, J. Tian, G. Huang, J. Bi and L. Wu, Rational design of novel COF/MOF S-scheme hetero-junction photocatalyst for boosting CO_2 reduction at gas–solid interface, *ACS Appl. Mater. Interfaces*, 2022, **14**, 24299–24308.

79 R.-G. Yang, Y.-M. Fu, H.-N. Wang, D.-P. Zhang, Z. Zhou, Y.-Z. Cheng, X. Meng, Y.-O. He and Z.-M. Su, ZIF-8/covalent organic framework for enhanced CO_2 photocatalytic reduction in gas–solid system, *Chem. Eng. J.*, 2022, **450**, 138040.

80 M. Yang, Y. Mao, B. Wang, L. Lin, Y. Wang, L. Zhang, Y. Jiang, M. Zhao, H. Chen and Y. Zhang, Heterometallic Mg@Fe-MIL-101/TpPa-1-COF grown on stainless steel mesh: Enhancing photo-degradation, fluorescent detection and toxicity assessment for tetracycline hydrochloride, *Colloids Surf., A*, 2021, **631**, 127725.

81 H.-L. Jiang, Q.-B. Fu, M.-L. Wang, J.-M. Lin and R.-S. Zhao, Determination of trace bisphenols in functional beverages through the magnetic solid-phase extraction with MOF-COF composite, *Food Chem.*, 2021, **345**, 128841.

82 L.-L. Zheng, L.-S. Zhang, Y. Chen, L. Tian, X.-H. Jiang, L.-S. Chen, Q.-J. Xing, X.-Z. Liu, D.-S. Wu and J.-P. Zou, A new strategy for the fabrication of covalent organic framework-metal–organic framework hybrids *via* in-situ functionalization of ligands for improved hydrogen evolution reaction activity, *Chin. J. Catal.*, 2022, **43**, 811–819.

83 P. Xue, X. Pan, T. Tian, M. Tang, W. Guo, J. Li, Z. Wang and H. Tang, Boosting photocatalytic hydrogen evolution of covalent organic frameworks by introducing 2D conductive metal–organic frameworks as noble metal-free co-catalysts, *Catal. Sci. Technol.*, 2022, **12**, 3158–3164.

84 S. Zhang, Q. Yang, X. Xu, X. Liu, Q. Li, J. Guo, N. L. Torad, S. M. Alshehri, T. Ahamad, M. S. A. Hossain, Y. V. Kaneti and Y. Yamauchi, Assembling well-arranged covalent organic frameworks on MOF-derived graphitic carbon for remarkable formaldehyde sensing, *Nanoscale*, 2020, **12**, 15611–15619.

85 S. Zhang, W. Xia, Q. Yang, Y. Valentino Kaneti, X. Xu, S. M. Alshehri, T. Ahamad, M. S. A. Hossain, J. Na, J. Tang and Y. Yamauchi, Core–shell motif construction: Highly graphitic nitrogen-doped porous carbon electrocatalysts using MOF-derived carbon@COF heterostructures as sacrificial templates, *Chem. Eng. J.*, 2020, **396**, 125154.

86 R. He, K. Xue, J. Wang, T. Yang, R. Sun, L. Wang, X. Yu, U. Omeoga, W. Wang, T. Yang, Y. Hu and S. Pi, Design and synthesis of La3 + -, Sb3 + -doped MOF-In2S3@FcDc-TAPT COFs hybrid materials with enhanced photocatalytic activity, *J. Mater. Sci.*, 2019, **54**, 14690–14706.

87 M.-L. Xu, J.-R. Li, X.-M. Wu, T. Yu, G.-Y. Qin, F.-J. Wang, L.-N. Zhang, K. Li and X. Cheng, The excellent photocatalytic overall water splitting activity of TpPa-1-COF excited *via*

88 MOF derived FeP-PC and α-Fe₂O₃ dual cocatalysts, *Appl. Surf. Sci.*, 2022, **602**, 154371.

88 Y. Li, J. Feng, Y. Zhang, C. Wang, J. Hao, Y. Wang, Y. Xu and X. Cheng, Covalent organic frameworks@ZIF-67 derived novel nanocomposite catalyst effectively activated peroxymonosulfate to degrade organic pollutants, *Chemosphere*, 2023, **311**, 137038.

89 Q. Miao, S. Yang, Q. Xu, M. Liu, P. Wu, G. Liu, C. Yu, Z. Jiang, Y. Sun and G. Zeng, Constructing synergistic Zn-N4 and Fe-N₄O dual-sites from the COF@MOF derived hollow carbon for oxygen reduction reaction, *Small Struct.*, 2022, **3**, 2100225.

90 T. Zhang, G. Xing, W. Chen and L. Chen, Porous organic polymers: a promising platform for efficient photocatalysis, *Mater. Chem. Front.*, 2020, **4**, 332–353.

91 G. Yuan, L. Tan, P. Wang, S. Feng, H. Tang, G. Wang, C. Wang and H. Yan, Graphene oxide modified UiO-66-NH₂/COF for promoting photocatalytic H_2 evolution, *Mater. Lett.*, 2022, **325**, 132863.

92 J. Ran, M. Jaroniec and S.-Z. Qiao, Cocatalysts in semiconductor-based photocatalytic CO2 reduction: Achievements, challenges, and opportunities, *Adv. Mater.*, 2018, **30**, 1704649.

93 D. Li, M. Kassymova, X. Cai, S.-Q. Zang and H.-L. Jiang, Photocatalytic CO_2 reduction over metal–organic framework-based materials, *Coord. Chem. Rev.*, 2020, **412**, 213262.

94 Y.-N. Gong, W. Zhong, Y. Li, Y. Qiu, L. Zheng, J. Jiang and H.-L. Jiang, Regulating photocatalysis by spin-state manipulation of cobalt in Covalent Organic Frameworks, *J. Am. Chem. Soc.*, 2020, **142**, 16723–16731.

95 K. Sun, Y. Qian and H.-L. Jiang, Metal–Organic Frameworks for photocatalytic water splitting and CO_2 reduction, *Angew. Chem., Int. Ed.*, 2023, **62**, e202217565.

96 J. Zhou, J. Li, L. Kan, L. Zhang, Q. Huang, Y. Yan, Y. Chen, J. Liu, S.-L. Li and Y.-Q. Lan, Linking oxidative and reductive clusters to prepare crystalline porous catalysts for photocatalytic CO_2 reduction with H_2O, *Nat. Commun.*, 2022, **13**, 4681.

97 X. Wang, G. Chang, C. Liu, R. Li, Y. Jin, X. Ding, X. Liu, H. Wang, T. Wang and J. Jiang, Chemical conversion of metal–organic frameworks into hemi-covalent organic frameworks, *Inorg. Chem. Front.*, 2022, **9**, 4776–4784.

98 L. Yao, Y. Hu, Y. Zou, Z. Ji, S. Hu, C. Wang, P. Zhang, H. Yang, Z. Shen, D. Tang, S. Zhang, G. Zhao and X. Wang, Selective and efficient photoextraction of aqueous Cr(vi) as a solid-state polyhydroxy Cr(v) complex for environmental remediation and resource recovery, *Environ. Sci. Technol.*, 2022, **56**, 14030–14037.

99 S. Li, Y. Hu, Z. Shen, Y. Cai, Z. Ji, X. Tan, Z. Liu, G. Zhao, S. Hu and X. Wang, Rapid and selective uranium extraction from aqueous solution under visible light in the absence of solid photocatalyst, *Sci. China: Chem.*, 2021, **64**, 1323–1331.

100 Y. Hu, D. Tang, Z. Shen, L. Yao, G. Zhao and X. Wang, Photochemically triggered self-extraction of uranium from aqueous solution under ambient conditions, *Appl. Catal., B*, 2023, **322**, 122092.

101 X. Zhong, Q. Ling, Z. Ren and B. Hu, Immobilization of U(VI) onto covalent organic frameworks with the different periodic structure by photocatalytic reduction, *Appl. Catal., B*, 2023, **326**, 122398.

102 H. Li, F. Zhai, D. Gui, X. Wang, C. Wu, D. Zhang, X. Dai, H. Deng, X. Su, J. Diwu, Z. Lin, Z. Chai and S. Wang, Powerful uranium extraction strategy with combined ligand complexation and photocatalytic reduction by post-synthetically modified photoactive metal–organic frameworks, *Appl. Catal., B*, 2019, **254**, 47–54.

103 V. Kumar, V. Singh, K.-H. Kim, E. E. Kwon and S. A. Younis, Metal–organic frameworks for photocatalytic detoxification of chromium and uranium in water, *Coord. Chem. Rev.*, 2021, **447**, 214148.

104 K. Yu, L. Tang, X. Cao, Z. Guo, Y. Zhang, N. Li, C. Dong, X. Gong, T. Chen, R. He and W. Zhu, Semiconducting Metal–Organic Frameworks decorated with spatially separated dual cocatalysts for efficient uranium(VI) photoreduction, *Adv. Funct. Mater.*, 2022, **32**, 2200315.

105 J.-Y. Yue, Y.-T. Wang, X.-L. Ding, Y.-F. Fan, L.-P. Song, P. Yang, Y. Ma and B. Tang, Single-atom substitution in donor–acceptor covalent organic frameworks for tunable visible light photocatalytic Cr(VI) reduction, *Mater. Chem. Front.*, 2022, **6**, 3748–3754.

106 X. Zhong, Y. Liu, W. Zeng, Y. Zhu and B. Hu, Excellent-photoreductionperformance of U(VI) on metal organic framework/covalent organic framework heterojunction by solar-driven, *Sep. Purif. Technol.*, 2022, **285**, 120405.

107 Z. Wu, X. Huang, X. Li, G. Hai, B. Li and G. Wang, Covalent-organic frameworks with keto–enol tautomerism for efficient photocatalytic oxidative coupling of amines to imines under visible light, *Sci. China: Chem.*, 2021, **64**, 2169–2179.

108 K. Zhang, F. Chu, Y. Hu, X. Huang, G. Zhao and G. Wang, Ce-doped MIL-125-NH$_2$ coupled Ce^{4+}/Ce^{3+} and Ti^{4+}/Ti^{3+} redox mediators for thermo-enhanced photocatalytic oxidative desulfurization, *Chin. Chem. Lett.*, 2023, **34**, 107766.

109 K. Feng, H. Hao, F. Huang, X. Lang and C. Wang, A 2D porphyrin-based covalent organic framework with TEMPO for cooperative photocatalysis in selective aerobic oxidation of sulfides, *Mater. Chem. Front.*, 2021, **5**, 2255–2260.

110 D. Wang, M. Wang and Z. Li, Fe-Based Metal–Organic Frameworks for Highly Selective Photocatalytic Benzene Hydroxylation to Phenol, *ACS Catal.*, 2015, **5**, 6852–6857.

111 L. Xiong and J. Tang, Strategies and challenges on selectivity of photocatalytic oxidation of organic substances, *Adv. Energy Mater.*, 2021, **11**, 2003216.

112 G. Lu, F. Chu, X. Huang, Y. Li, K. Liang and G. Wang, Recent advances in Metal–Organic Frameworks-based materials for photocatalytic selective oxidation, *Coord. Chem. Rev.*, 2022, **450**, 214240.

113 Z. Wu, K. Zhang, X. Li, G. Hai, X. Huang and G. Wang, Conjugated polymer coated MIL-125(Ti) as an efficient photocatalyst for selective oxidation of benzylic CH bond under visible light, *Appl. Surf. Sci.*, 2021, **555**, 149732.

114 X. Li, J. Wang, F. Xue, Y. Wu, H. Xu, T. Yi and Q. Li, An Imine-linked Metal–Organic Framework as a reactive oxygen species generator, *Angew. Chem., Int. Ed.*, 2021, **60**, 2534–2540.

115 Z. Wu, X. Huang, H. Zheng, P. Wang, G. Hai, W. Dong and G. Wang, Aromatic heterocycle-grafted NH2-MIL-125(Ti) *via* conjugated linker with enhanced photocatalytic activity for selective oxidation of alcohols under visible light, *Appl. Catal., B*, 2018, **224**, 479–487.

116 X. Huang, X. Li, W. Xia, B. Hu, M. Muhler and B. Peng, Highly dispersed Pd clusters/nanoparticles encapsulated in MOFs *via* in situ auto-reduction method for aqueous phenol hydrogenation, *J. Mater. Sci. Technol.*, 2022, **109**, 167–175.

117 Z. Chen, Y. Li, Y. Cai, S. Wang, B. Hu, B. Li, X. Ding, L. Zhuang and X. Wang, Application of covalent organic frameworks and metal–organic frameworks nanomaterials in organic/inorganic pollutants removal from solutions through sorption-catalysis strategies, *Carbon Res.*, 2023, **2**, 8.

118 G. Liu, Z. Dai, X. Liu, R. A. Dahlgren and J. Xu, Modification of agricultural wastes to improve sorption capacities for pollutant removal from water – a review, *Carbon Res.*, 2022, **1**, 24.

119 H. Chen, Y. Gao, J. Li, Z. Fang, N. Bolan, A. Bhatnagar, B. Gao, D. Hou, S. Wang, H. Song, X. Yang, S. M. Shaheen, J. Meng, W. Chen, J. Rinklebe and H. Wang, Engineered biochar for environmental decontamination in aquatic and soil systems: a review, *Carbon Res.*, 2022, **1**, 4.

120 J. He, W. Ma, L. Han, L. Chen, E. G. Xu, B. Xing and Z. Yang, Unraveling the role of natural and pyrogenic dissolved organic matter in photodegradation of biodegradable microplastics in freshwater, *Carbon Res.*, 2023, **2**, 18.

121 Y. Luo, Y. Zhu, Y. Han, H. Ye, R. Liu, Y. Lan, M. Xue, X. Xie, S. Yu, L. Zhang, Z. Yin and B. Gao, g-C$_3$N$_4$-based photocatalysts for organic pollutant removal: a critical review, *Carbon Res.*, 2023, **2**, 14.

122 Y. Xue, G. Zhao, R. Yang, F. Chu, J. Chen, L. Wang and X. Huang, 2D metal–organic framework-based materials for electrocatalytic, photocatalytic and thermocatalytic applications, *Nanoscale*, 2021, **13**, 3911–3936.

123 X. Hu, J. Bao, D. Chen, S. Jalil Shah, S. Subhan, W. Gong, W. Li, X. Luan, Z. Zhao and Z. Zhao, Accelerating the Fe(III)/Fe(II) cycle *via* enhanced electronic effect in NH2-MIL-88B(Fe)/TPB-DMTP-COF composite for boosting photo-Fenton degradation of sulfamerazine, *J. Colloid Interface Sci.*, 2022, **624**, 121–136.

124 X. Guo, D. Yin, K. K. Khaing, J. Wang, Z. Luo and Y. Zhang, Construction of MOF/COF hybrids for boosting sunlight-induced Fenton-like photocatalytic removal of organic pollutants, *Inorg. Chem.*, 2021, **60**, 15557–15568.

125 Y. Li, L. Liu, T. Meng, L. Wang and Z. Xie, Structural engineering of ionic MOF@COF heterointerface for exciton-boosting sunlight-driven photocatalytic filter, *ACS Nano*, 2023, **17**, 2932–2942.

126 Z. Wu, Y. Li, C. Zhang, X. Huang, B. Peng and G. Wang, Recent advances in metal–organic-framework-

based catalysts for thermocatalytic selective oxidation of organic substances, *Chem. Catal.*, 2022, **2**, 1009–1045.

127 D. Zhao, X. Li, K. Zhang, J. Guo, X. Huang and G. Wang, Recent advances in thermocatalytic hydrogenation of unsaturated organic compounds with Metal–Organic Frameworks-based materials: Construction strategies and related mechanisms, *Coord. Chem. Rev.*, 2023, **487**, 215159.

128 M. Ding and H.-L. Jiang, Incorporation of imidazolium-based poly(ionic liquid)s into a Metal–Organic Framework for CO_2 capture and conversion, *ACS Catal.*, 2018, **8**, 3194–3201.

129 Q. Sun, B. Aguila, J. A. Perman, T. Butts, F.-S. Xiao and S. Ma, Integrating superwettability within Covalent Organic Frameworks for functional coating, *Chem*, 2018, **4**, 1726–1739.

130 X. Huang, K. Zhang, B. Peng, G. Wang, M. Muhler and F. Wang, Ceria-based materials for thermocatalytic and photocatalytic organic synthesis, *ACS Catal.*, 2021, **11**, 9618–9678.

131 Q. Yang, Y.-Z. Chen, Z. U. Wang, Q. Xu and H.-L. Jiang, One-pot tandem catalysis over Pd@MIL-101: boosting the efficiency of nitro compound hydrogenation by coupling with ammonia borane dehydrogenation, *Chem. Commun.*, 2015, **51**, 10419–10422.

132 P. Falcaro, R. Ricco, A. Yazdi, I. Imaz, S. Furukawa, D. Maspoch, R. Ameloot, J. D. Evans and C. J. Doonan, Application of metal and metal oxide nanoparticles@-MOFs, *Coord. Chem. Rev.*, 2016, **307**, 237–254.

133 M. Zhao, K. Yuan, Y. Wang, G. Li, J. Guo, L. Gu, W. Hu, H. Zhao and Z. Tang, Metal–organic frameworks as selectivity regulators for hydrogenation reactions, *Nature*, 2016, **539**, 76–80.

134 K. Choe, F. Zheng, H. Wang, Y. Yuan, W. Zhao, G. Xue, X. Qiu, M. Ri, X. Shi, Y. Wang, G. Li and Z. Tang, Fast and selective semihydrogenation of alkynes by palladium nanoparticles sandwiched in Metal–Organic Frameworks, *Angew. Chem., Int. Ed.*, 2020, **59**, 3650–3657.

135 B. Chen, X. Yang, Y. Xu, S. Hu, X. Zeng, Y. Liu, K. B. Tan, J. Huang and G. Zhan, Semi-hydrogenation of α,β-unsaturated aldehydes over sandwich-structured nanocatalysts prepared by phase transformation of thin-film Al_2O_3 to Al-TCPP, *Nanoscale*, 2022, **14**, 15749–15759.

136 M.-L. Gao, L. Li, Z.-X. Sun, J.-R. Li and H.-L. Jiang, Facet engineering of a Metal–Organic Framework support modulates the microenvironment of palladium nanoparticles for selective hydrogenation, *Angew. Chem., Int. Ed.*, 2022, **61**, e202211216.

137 K. Liu, S. Jiao, H. Zhao, F. Cao and D. Ma, Hybridization of MOFs and ionic POFs: a new strategy for the construction of bifunctional catalysts for CO_2 cycloaddition, *Green Chem.*, 2021, **23**, 1766–1771.

138 Z. Rafiee, Fabrication of efficient Zn-MOF/COF catalyst for the Knoevenagel condensation reaction, *J. Iran. Chem. Soc.*, 2021, **18**, 2657–2664.

139 B. Parmar, P. Patel, V. Murali, Y. Rachuri, R. I. Kureshy, N.-U. H. Khan and E. Suresh, Efficient heterogeneous catalysis by dual ligand Zn(II)/Cd(II) MOFs for the Knoevenagel condensation reaction: adaptable synthetic routes, characterization, crystal structures and luminescence studies, *Inorg. Chem. Front.*, 2018, **5**, 2630–2640.

140 M. D. M. Darder, S. Salehinia, J. B. Parra, J. M. Herrero-Martinez, F. Svec, V. Cerdà, G. Turnes Palomino and F. Maya, Nanoparticle-directed Metal–Organic Framework/porous organic polymer monolithic supports for flow-based applications, *ACS Appl. Mater. Interfaces*, 2017, **9**, 1728–1736.

141 M.-H. Qi, M.-L. Gao, L. Liu and Z.-B. Han, Robust bifunctional core–shell MOF@POP catalyst for one-pot tandem reaction, *Inorg. Chem.*, 2018, **57**, 14467–14470.

142 E. Rahmati and Z. Rafiee, Synthesis of Co-MOF/COF nanocomposite: application as a powerful and recoverable catalyst in the Knoevenagel reaction, *J. Porous Mater.*, 2021, **28**, 19–27.

143 Y. Zhang, L. Liu, W.-G. Xu and Z.-B. Han, MOF@POP core–shell architecture as synergetic catalyst for high-efficient CO_2 fixation without cocatalyst under mild conditions, *J. CO2 Util.*, 2021, **46**, 101463.

144 G. Lu, H. Zheng, J. Lv, G. Wang and X. Huang, Review of recent research work on CeO_2-based electrocatalysts in liquid-phase electrolytes, *J. Power Sources*, 2020, **480**, 229091.

145 P. Zhou, G. Hai, G. Zhao, R. Li, X. Huang, Y. Lu and G. Wang, CeO2 as an "electron pump" to boost the performance of Co4N in electrocatalytic hydrogen evolution, oxygen evolution and biomass oxidation valorization, *Appl. Catal., B*, 2023, **325**, 122364.

146 G. Zhao, G. Hai, P. Zhou, Z. Liu, Y. Zhang, B. Peng, W. Xia, X. Huang and G. Wang, Electrochemical oxidation of 5-hydroxymethylfurfural on CeO_2-modified Co_3O_4 with regulated Intermediate adsorption and promoted charge transfer, *Adv. Funct. Mater.*, 2023, **33**, 2213170.

147 X. Cui, S. Lei, A. C. Wang, L. Gao, Q. Zhang, Y. Yang and Z. Lin, Emerging covalent organic frameworks tailored materials for electrocatalysis, *Nano Energy*, 2020, **70**, 104525.

148 T. Wang, C. Yang, Y. Liu, M. Yang, X. Li, Y. He, H. Li, H. Chen and Z. Lin, Dual-shelled multidoped hollow carbon nanocages with hierarchical porosity for high-performance oxygen reduction reaction in both alkaline and acidic media, *Nano Lett.*, 2020, **20**, 5639–5645.

149 T. Wang, Y. He, Y. Liu, F. Guo, X. Li, H. Chen, H. Li and Z. Lin, A ZIF-triggered rapid polymerization of dopamine renders Co/N-codoped cage-in-cage porous carbon for highly efficient oxygen reduction and evolution, *Nano Energy*, 2021, **79**, 105487.

150 P. Zhou, J. Lv, X. Huang, Y. Lu and G. Wang, Strategies for enhancing the catalytic activity and electronic conductivity of MOFs-based electrocatalysts, *Coord. Chem. Rev.*, 2023, **478**, 214969.

151 S. Huang, K. Chen and T.-T. Li, Porphyrin and phthalocyanine based covalent organic frameworks for electrocatalysis, *Coord. Chem. Rev.*, 2022, **464**, 214563.

152 R. Madhu, A. Karmakar, K. Bera, S. Nagappan, H. N. Dhandapani, A. De, S. S. Roy and S. Kundu, Recent developments in transition metal-based MOFs for electrocatalytic water splitting emphasizing fundamental and structural aspects, *Mater. Chem. Front.*, 2023, **7**, 2120–2152.

153 S. Meng, G. Li, P. Wang, M. He, X. Sun and Z. Li, Rare earth-based MOFs for photo/electrocatalysis, *Mater. Chem. Front.*, 2023, **7**, 806–827.

154 Z. Meng, N. Chen, S. Cai, R. Wang, J. Wu and H. Tang, Recent advances of hierarchically porous bifunctional oxygen electrocatalysts derived from metal–organic frameworks for Zn–air batteries, *Mater. Chem. Front.*, 2021, **5**, 2649–2667.

155 W. Li, C. Han, K. Zhang, S. Chou and S. Dou, Strategies for boosting carbon electrocatalysts for the oxygen reduction reaction in non-aqueous metal–air battery systems, *J. Mater. Chem. A*, 2021, **9**, 6671–6693.

156 W. Xue, Q. Zhou, X. Cui, S. Jia, J. Zhang and Z. Lin, Metal–organic frameworks-derived heteroatom-doped carbon electrocatalysts for oxygen reduction reaction, *Nano Energy*, 2021, **86**, 106073.

157 Q. Xu, Y. Tang, X. Zhang, Y. Oshima, Q. Chen and D. Jiang, Template conversion of Covalent Organic Frameworks into 2D conducting nanocarbons for catalyzing oxygen reduction reaction, *Adv. Mater.*, 2018, **30**, 1706330.

158 N. Kornienko, Operando spectroscopy of nanoscopic metal/covalent organic framework electrocatalysts, *Nanoscale*, 2021, **13**, 1507–1514.

159 H. Park, O. Kwon and J. Kim, Computational identification of connected MOF@COF materials, *J. Phys. Chem. C*, 2021, **125**, 5897–5903.